A two-year long drought in summer 2014/2015 and 2015/2016 over South Africa

by Bellinda Monyela

Minor dissertation presented in the partial fulfilment of the requirements for the Master's degree of Ocean and Atmospheric Sciences.

Department of Oceanography, University of Cape Town

April 2017

Plagiarism Declaration

I, Bellinda Mashoene Monyela, declare that the contents of this thesis represent my own unaided work, and that the thesis has not previously been submitted for academic examination towards any qualification. Furthermore, it represents my own opinions and not necessarily those of the University of Cape Town.

Date: 17/04/2017

Signed: BM Monyela

Signed by candidate

Signature Removed

Dedication

This dissertation is dedicated to my mom and my two nieces Amogelang and Atlegang. To my angel in heaven, my Dad, I hope you are very happy and proud of your little girl; I am almost there to fulfil my promise. To: Bonolo, Cia, Phashana and Epeleng, I wouldn't trade your sisterhood and brotherhood for anything, this is for you!

Go wena Modimo, Ramasedi wa poloko, ke leboga lerato, boitshepo, hlotloletso le kgothatso tseo o nkapesitsego tsona ka matsatsi ohle. Tumisho le theto a di ye go wena ka mehla yohle.Go lena baga Matheba, Phasha, Malatji, dinoko, baga Monyela didiba, dikgomo tsa lala lelenyora, kgadi ya ga Mmalegapa' a makgolo, o re montshepetsa boshego re mo leboga go sele.

Moshate!!!

Acknowledgements

The financial assistance from WRC, NRF, UCT Postgraduate Funding and ACCESS towards this thesis is highly appreciated. I am grateful to my supervisor, Professor Mathieu Rouault for the academic advice. I would like to thank SAWS for providing the data. I would also like to thank Rodrigue, Arielle, Ramontsheng and Georges-Noel for the technical assistance through Matlab and constant advice on my thesis. To my mentors: Paballo Chauke, Malebogo Ngoepe, Natalie Ragoasha and Phililе Mbatha, I thank you for holding me when I tripped, limped, fell and for celebrating me when I didn't have a reason to. Elaine Martin and Dr Cathy Van Der Westhuizen, thanks for your free services. I survived this because of you; I appreciate everything you did for me. Ngwanapapa, Lillian Maboya, your motivation and courage kept me going. Matsubu, Mahiine, Mamateane, Aquinar, Koketso and Makhi, thanks for encouraging me during my weakest days and nights. Lastly, the children of the soil from the Oceanography Department, your love, support, debates and your laughter kept me going.

Abstract

Droughts occurred over South Africa during the summer seasons of 2014/2015 and 2015/2016. At the same time, the Pacific Ocean was warmer than normal starting in 2014 and leading to the very strong 2015/2016 El Niño. The first objective of this study is to document the ocean and climate conditions that occurred during the summer seasons 2014/2015 and 2015/2016 in southern Africa. NCEP Reanalysis data is used to compute the monthly and seasonal scale composite mean and anomalies of large-scale circulations during the summer seasons of 2014/2015 and 2015/2016. Results obtained from the study suggest that some months of 2014/2015 and 2015/2016 were canonical to the effect of El Niño over southern Africa, but not all of them during the summer seasons were dry. The wetter than normal conditions in northeast South Africa, Botswana and Zimbabwe during December 2014 are unfamiliar for a canonical summer El Niño event over southern Africa. Anomalous cooler than normal Sea Surface Temperature (SST) occurred over the west coast and south coast during December 2014 and February 2015, while it is usually warmer during El Niño. Additionally, the colder than normal SST at the south coast during February 2016 and Namibian and West Coast during March 2016 does not mimic the canonical El Niño patterns. However, this did not influence the El Niño-like warmer seasonal SST average during 2015/2016. The lower than normal pressure anomalies over the subcontinent during December 2014 and January 2015 were not portraying a canonical El Niño pattern but the other months were. The seasonal larger than normal pressure at 500 hPa over the subcontinent was more typical of El Niño during summer 2015/2016 and acted to suppress rainfall. Secondly, the study uses the Standard Precipitation Index (SPI) at different time scales (3 months duration, 5 months duration and 17 months duration) to assess the severity of 2015/2016 summer drought compared to the other droughts of the 20^{th} and 21^{st} century (1921 to 2016) and to analyse the relationship between droughts and ENSO. The South African Weather Service (SAWS) rainfall data shows that KwaZulu-Natal was the only region within South Africa, to have the 2015/2016 as the strongest summer drought since 1921 but 2015/2016 was still one of the worst droughts on record in South Africa, especially at the 2 consecutive seasonal scales. In general, droughts are favored by El Niño and wetter conditions by La Niña, but the second strongest El Niño of 1997/1998 led to near normal rainfall over the north-eastern region at all time-scales. The SPI has proven to be very versatile, flexible and very effective to monitor the 2015/2016 summer drought in the complex South African rainfall regime. However, there was little difference between 3 months SPI at the end of February and 5 months SPI at the end of March. For South Africa, the summer rainfall 2015/2016 season had the fifth worst drought after El Niño related drought of 1982/1983 and 1991/1992 and the non-El Niño related droughts of 1967/1968 and 1944/1945. At the 17-month scale, an index that encompasses two summer seasons 2015/2016 was the third worst drought since summer 1921/1922 due to dry conditions in 2014/2015 and 2015/2016.

Contents

Plagiarism Declaration 2
Dedication 3
Acknowledgements 4
Abstract 5
List of figures 8
List of table 10
Abbreviations 11
1. Introduction 12
2. Literature Review 12
2.1. Southern African Climate 12
2.2. Atmospheric circulation over southern Africa during austral summer 13
2.3. South African Rainfall bearing systems 14
2.4. Local and Remote Influence of Oceans on Southern African rainfall 15
2.5. Droughts 17
3. Data and Methods. 18
3.1. Atmospheric circulations 18
3.2. Nino 3.4 Index 18
3.3. SPI data 18
4. Results and Discussion 19
4.1. Rainfall over southern Africa 19
4.2. Sea Surface Temperature 24
4.3. Geopotential height at 1000 hPa 28
4.4. Geopotential height at 500 hPa 32
4.5. Rainfall climatology 37
4.6. El Niño Index. 38
4.7. South African subdomains and SPI 40
5. Conclusion 44
Appendix A 46
Appendix B 49
References 51

List of figures

Figure 1: Location of the 94 rainfall districts of the SAWS. The 94 districts are further categorised into 8 homogenous rainfall area defined by SAWS, namely: North-Western Cape (1), South-Western Cape (2), South Coast (3), Southern Interior (4), Western Interior (5), Central Interior (6), Kwa-Zulu Natal (7) and North-Eastern Interior (8). (Rouault and Richard 2003). 19

Figure 2 : Global rainfall (mm/ day) El Niño composite anomaly from climatology from December 1982 to March 2016 using GPCP data. A positive (negative) anomaly implies wetter (drier) than normal rainfall. El Niño years considered were 1983, 1987, 1992, 1995,1998, 2002, 2005, 2007 ,2010, 2015 and 2016. 20

Figure 3 : Top left El Niño composite of rainfall anomalies (mm/day) from Dec1983 to Mar 2016 for Southern Africa. Top right: same for 2014/2015 summer and, bottom: 2015/2016 summer (c). Positive anomalies mean wetter than normal rainfall and negative anomalies mean drier than normal rainfall..... 21

Figure 4: From top to bottom and left to right: rainfall anomalies (mm/day) from climatology over Southern Africa during the summer season 2014/2015 (a) December 2014 (b) January 2015 (c) February2015 and (d) March 2015. Positive (negative) anomalies indicate wetter (drier) than normal rainfall..... 22

Figure 5: From top to bottom and left to right: rainfall anomalies (mm/day) from climatology over Southern African during the summer season 2015/2016 (a) December 2015 (b) January 2016 (c) February 2016 and (d) March 2016. Positive (negative) anomalies indicate wetter (drier) than normal rainfall..... 23

Figure 6: Global SST (^{0}C) composite anomaly from climatology for the summer season from December 1982 to March 2016) using NOAA OI SST data during El Niño years. Positive(negative) anomalies indicate warmer (colder) than normal SST. El Niño years considered were 1983, 1987, 1992, 1995, 1998, 2002, 2005, 2007, 2010, 2015 and 2016..... 24

Figure 7 : Composite of SST anomalies (^{0} C) during El Niño for the summer season from Dec 1983 to Mar 2016 for southern Africa (a, top left), (b, top right) 2014/2015 and 2015/2016 (c, bottom). Positive anomalies means warmer than normal SST and negative anomalies mean colder than normal SST.. 25

Figure 8: SST anomalies (^{0} C) from climatology over southern African during the summer season 2014/2015. (a) December 2014 (b) January 2015 (c) February 2015 and (d) March 2015. Positive (negative) anomalies indicate warmer (colder) than normal SST..... 26

Figure 9: SST anomalies (^{0}C) from climatology over southern African during the summer season 2015/2016. (a) December 2015 (b) January 2016 (c) February 2016 and (d) March 2016. Positive (negative) anomalies indicate warmer (colder) than normal SST..... 27

Figure 10: Composite for geopotential height anomaly (m) for the summer season during El Niño years from December 1982 to March 2016 at 1000 hPa. Positive anomalies indicate

higher than normal pressure and negative anomalies indicate lower than normal pressure. El Niño years considered were 1983, 1987, 1992, 1995, 1998, 2002, 2005, 2007, 2010, 2015. 28

Figure 11: Top left: composite of 1000 hPa geopotential height anomaly (m) during El Niño for the summer season Dec 1982 to Mar 2016 for southern African (a), Top right 2014/2015 (b) and bottom 2015/2016 (c). Positive anomalies mean higher than normal pressure and negative anomalies mean lower than normal pressure. 29

Figure 12 : 1000 hPa geopotential height anomalies (m) during summer season (December 2014-March 2015) over Southern Africa at 1000 hPa. (a)December 2014, (b) January 2015, (c) February 2015 and (d) March 2015. Positive anomalies mean higher than normal pressure and negative anomalies mean lower than normal pressure. 30

Figure 13: Geopotential height anomalies (m) during summer season (December 2015- March 2016) over southern African at 1000 hPa. (a) December 2015, (b) January 2016, (c) February 2016 and (d) March 2016. 32

Figure 14: The composite anomaly for geopotential height for El Niño summers at 500 hPa. Positive anomalies imply higher than normal pressure while negative anomalies imply lower than normal pressure. El Niño years considered were 1983, 1987, 1992, 1995, 2003, 2005,2007, 2010, 2015 and 2016. 33

Figure 15 : Geopotential height anomalies (m) during summer season (December 2015- March 2016) over southern African at 500 hPa. (a) December 2015, (b) January 2016, (c) February 2016 and (d) March 2016 34

Figure 16 : Geopotential height anomalies (m) during the 2014/2015 summer season over southern Africa at 500 hPa. (a)December 2014, (b) January 2015, (c) February 2015 and (d) March 2015. 35

Figure 17: Geopotential height anomalies (m) during the 2015/2016 summer season over southern African at 500 hPa. (a) December 2015, (b) January 2016, (c) February 2016 and (d) March 2016. 36

Figure 18: Monthly rainfall mean (mm/month) for the 8-homogenous area defined by SAWS from 1921 to 2016. 37

Figure 19 : Nino 3.4 index. Red and blue bars represent El Niño and La Niña respectively, while the black bars represent a neutral year. ENSO episodes are defined from summer of 1921 to 2016. .. 39

Figure 20: SPI at 3, 5 and 17 month time scale at the end of February for 3 month and March for 5 and 17 month for summer rainfall region. 39

Figure 21: SPI at 3, 5 and 17-months' time scale at the end of February for 3 month and March for 5 and 17 months for Central Interior. 41

Figure 22: SPI at 3, 5 and 17-month time scale at the end of February for 3 month and March for 5 and 17-months for KwaZulu- Natal. 41

Figure 23: SPI at 3, 5 and 17-month time scale at the end of February for 3 month and March for 5 and 17 month for northern Interior 42

Figure 24: SPI at 3, 5 and 17-months' time scale at the end of February for 3 month and March for 5 and 17-month for southern Interior. 43

Figure 25: SPI at 3, 5 and 17-month time scale at the end of February for 3 month and March for 5 and 17 months for western Interior 44

List of table

Table 1: The classification of the SPI values 40

Abbreviations

AVHRR Advanced Very High-Resolution Radiometer

ASCII American Standard Code for Information Interchange

ENSO El Niño Southern Oscillation

ERSST Extended Reconstruction Sea Surface Temperature

ESRL Earth System Research Laboratory

EOF Empirical Orthogonal Function

GPCP Global Precipitation Climatology Centre

ITCZ Inter-Tropical Convergence Zone

MCCs Meso-scale Convective Complexes

NOAA National Oceanic and Atmospheric Administration

NCEP National Centers for Environmental Prediction

OI Optimum Interpolation

SAA South Atlantic Anticyclone

SAWS South African Weather Service

SICZ South Indian Convergence Zone

SLP Sea Level Pressure

SOI Southern Oscillation Index

SO Southern Oscillation

SPI Standardized Precipitation Index

SST Sea Surface Temperature

SWIO South West Indian Ocean

TTT Tropical Temperate Troughs

WMO World Meteorological Organization

1. Introduction

Drought is one of the natural hazards that are prone to South Africa. Due to its high degree of spatiotemporal rainfall variability, South Africa experiences recurrent wet and dry spells (Cretat et al., 2012). The population of the country relies on the dual agricultural economy with both the rural subsistence and commercial farmers depending on rainfall for their livelihoods. Therefore, negative departures in the seasonal rainfall anomalies are accountable towards devastating droughts that have regional and national socio-economic impacts (Meque and Abiodun, 2014).

It has been established that the El Niño Southern Oscillation (ENSO) plays a significant role in the inter-annual rainfall variability in South Africa. Even though the relationship between ENSO and southern African rainfall is not linear, droughts in this region are usually found to be linked to El Niño events, while wetter than normal conditions are more associated with La Niña events (Rouault and Richard, 2003; Cretat et al., 2012; Meque and Abiodun, 2014). The relationship is found to be strongest during the summer peak rainfall months (Dieppois et al., 2015), and over the northern and south-eastern parts of South Africa (Richard et al., 2001). During the El Niño droughts, anomalous low-level divergence dominates the subcontinent and is also associated with higher than normal pressure in the troposphere, acting to prevent the advection of moisture on the continent and to suppress rainfall (Mason, 1994; Dieppois et al., 2015).

During the summer of 2015/2015 and 2015/2016, a severe drought affected the southern Africa continent. At the same time, warm anomalies developed in 2014 in the Pacific Ocean and conditions in austral summer 2014/2015 was nearly El Niño-like while one of the strongest El Niño developed in 2015. In general, the drought lasted for about 2 years. Due to crop failure, it has left 2.5 million of people in Malawi, Zimbabwe, Mozambique, Madagascar and Lesotho requiring quick humanitarian response while South Africa had a drop of 25 % in maize production in summer 2014/2015 (AgriSA, 2016). The first objective of the study is to investigate the atmospheric and oceanic conditions that have prevailed during summer 2014/2015 and 2015/2016 over southern Africa.

The second objective is to use the Standard Precipitation Index (SPI) used previously by Rouault and Richard (2003) to quantify whether the droughts of 2014/2015 and 2015/2016 were the strongest on record in South Africa compared to other droughts since 1921/1922. This study is divided into five chapters: chapter 2 contains the literature review; chapter 3 describes the data and methods, while results are found in chapter 4 and concluding remarks at chapter 5.

2. Literature Review

2.1. Southern African Climate

Southern Africa, a semi-arid region situated south of 15^0S of the equator experiences different climatic range. The difference is brought by the position of the subcontinent between the mid-latitudes and the tropics, different oceanic surrounding and topography (The Drakensberg, central plain and western escarpment). The outlined factors above lead to different climatic patterns and considerable spatiotemporal rainfall variability. For instance, most of the regions within this subcontinent experience rainfall during austral summer, while the South Coast receives rainfall all year round. The West Coast and the nearby hinterland are classified as austral winter rainfall region (Philippon et al., 2012). Rainfall is of high importance to the communities living within the summer rainfall zone because they depend on it for agricultural

purposes. Deviations from seasonal means, especially droughts affect the societal functioning and economy. Hence, understanding the atmospheric circulation in relation with factors allowing seasonal forecast such as El Niño or other climatic modes as antecedent conditions are significant in forecasting, mitigating and monitoring droughts.

2.2. Atmospheric circulation over southern Africa during austral summer

Southern Africa's climate and weather are influenced by the circulation systems that prevail in both the tropics to the south and temperate latitudes (Tyson and Preston-Whyte, 2000). However, the major atmospheric feature affecting this region is the semi-permanent, subtropical high-pressure systems (Tyson and Preston-Whyte, 2000). South Atlantic Anticyclone (SAA) lies at the southern part of the Atlantic Ocean and shifts latitudinally about 6^0 between seasons (Tyson and Preston-Whyte, 2000). SAA ridges around the southern part of the African continent usually producing onshore flow along the south and south-east coasts of South Africa (Blamey, 2012). Seasonal positional fluctuations in this anticyclone drive changes in the surface winds (Driver, 2014) as well as the Sea Surface Temperature (SST) around the Atlantic region (Reason, 2015). During austral summer, strong upwelling occurs along the west coast of southern Africa and throughout the year in South Africa and Namibia which is associated with colder SSTs influenced by the southerly winds around the SAA. Historically, little work has been undertaken to study the influence of South Atlantic on the southern African climate (Reason et al., 2006; Rouault et al., 2003), but its cold SST may not be strong enough to directly influence the southern African climate. The pronounced seasonal difference in southern Africa has been attributed to the variability of the Inter-Tropical Convergence Zone (ITCZ) and the annual cycle in the SAA (Reason, 2015). In austral summer, a strong relationship exists between the winds over the tropical south-east Atlantic and the convection in the Angola Low, highlighting the importance of this oceanic region on rainfall variability over subtropical southern Africa (Reason et al., 2006).

Reason and Jagadheesha (2005) demonstrated that the enhanced westerly winds off the south-east Atlantic towards the Angola Low are often associated with the wet conditions over the interior of the subcontinent. The other major feature that influences the rainfall of southern Africa is the Angola Low. The Angola Low is a semi-permanent, shallow heat low, located over southern Angola and northern Namibia. It is found to dominate the lower to mid-troposphere circulation over southern Africa during austral summer (Reason et al, 2006 and Hart et al, 2010). The Angola Low starts developing in October and strengthens towards January and February. During its development, neighbouring oceans and the weak surface high over southern Mozambique help to enhance the pressure gradient across Botswana and Zimbabwe (Hart et al., 2010). The generated pressure gradient, therefore, sets up the strong low-level north-easterly flow by promoting the flow of tropical easterlies north of Madagascar deep into the subcontinent (Hart et al., 2010). Mulenga (1999) suggested that the cold coastal temperatures from the Benguela upwelling region and the heated plateau over Angola contribute to this meridional temperature gradient. The Angola Low is documented as the primary driver of tropical moisture that assists with the development of the cloud bands by sustained moisture transport (Mulenga, 1999). Reason et al. (2006) further suggested that Angola Low and the SST in the tropical south-east Atlantic SST may significantly influence summer rainfall over large parts of subtropical Southern Africa namely Angola, Namibia and sometimes South Africa. Increased near surface westerlies observed off the tropical southeast to northwest Atlantic feeds a stronger Angola Low, leading to more low-level moisture in the source region of the tropical-temperate troughs (TTT) cloud bands (explained further in detail at 2.3.1) and it is vice versa with the decreased near surface westerlies (Reason et al., 2006). Meanwhile, at the tropical eastern equatorial Atlantic during austral summer, a warm pool of SST develops and feeds moisture in the Congo Basin and Angola, where strong land-based convection canonically occurs (Reason et al., 2006; Reason, 2015). The moisture produced from the warm pool region is the secondary source of moisture over the southern African rainfall region (Reason, 2015). The moisture flux becomes significant during the austral summer wet spells when it feeds into the Angola Low (Reason, 2015).

2.3. South African Rainfall bearing systems

Large-scale synoptic systems which produce convection are known to influence the summer rainfall of southern Africa (Tyson and Preston-Whyte, 2000). The rain-bearing systems are often produced by the disturbances in the general circulation southward of mid-latitudes to south and north of the tropics (Blamey, 2012).

2.3.1. Tropical Temperate Troughs

Hart et al. (2010) emphasized that cloud bands produced from tropical to extra tropical interactions are a common feature in many regions of the world, presented as an elongated region of cloudiness: established in the tropics, extends polewards and eastward into the mid-latitudes. Over southern Africa, canonical cloud bands commonly known as TTT are major synoptic rain-bearing system during summer (Hart et al., 2010). TTT are characterised by the presence of convection, rainfall and cloud bands elongated in NW-SE direction that links upper-tropospheric frontal system embedded in the mid-latitude westerly circulation with a tropical disturbance over the subcontinent (Fauchereau et al., 2009 and Cretat et al., 2012). The TTTs are not only known to produce the high-frequency rainfall variability over southern Africa (Tyson and Preston-Whyte, 2000 and Dube, 2002) but are also known to produce heavy rainfall events (Blamey, 2012). Usman and Reason (2004) documented that in some seasons when the tropical source is over the eastern margins of the subcontinent or Madagascar the TTT tends to be located further east. During these conditions, most of the southern African regions tend to experience significantly reduced rainfall (Reason and Jagadheesha, 2005). Fauchereau et al. (2009) emphasized that southern Africa and the South West Indian Ocean (SWIO) are one of only three preferred regions in the Southern Hemisphere for the occurrence of TTT. South Indian Convergence Zone (SICZ) has been suggested to exist as a region of convergence zone within the eastern region of the subcontinent and extending towards the southwest Indian Ocean (Cook, 2000). The TTT develops by establishing the connection between the mid-latitudes and the tropics at the SICZ (Dube, 2002).

2.3.2. Mesoscale Convective Complexes

The mesoscale rain bearing systems consists of phenomena such as tornadoes, thunderstorms and mesoscale convective complex (MCCs). Blamey and Reason (2013) discussed the role of organized MCC on the summer rainfall of southern Africa. MCCs are found to contribute up to 20% of the total summer rainfall (November-March) in the eastern parts of South Africa (Blamey and Reason, 2013). Even though the mechanism behind the production of MCC is still complex, MCC system like other convective system within this category are associated with extreme weather events (e.g. floods) and sometimes offer a relief to drought prone areas by increasing the seasonal averages (Blamey and Reason,2012). Thunderstorms are also a predominant feature of the summer rainfall, owing to the strong influence of diurnal heating and atmospheric instability (Tyson and Preston-Whyte,2000). Furthermore, due to orography and the warm Agulhas current, Rouault (2013) found out that summer rainfall in South Africa follows a diurnal cycle. Generally, maximum precipitation tends to occur in the late afternoon or early evening over land and early morning above the ocean near warm waters (Tyson and Preston-Whyte, 2000 and Rouault et al., 2013). The other summer rain-bearings systems of which will not be discussed in detail around southern Africa can be attributed to tropical cyclones (affecting the easternmost regions of southern Africa) and summer cut-off lows usually embedded within cloud bands (Harrison, 1984).

2.4. Local and Remote Influence of Oceans on Southern African rainfall

Southern Africa is positioned between the Indian and Atlantic Ocean. The spatial and seasonal distribution of rainfall is linked to its interaction with these surrounding oceans (Blamey and Reason, 2013). Indian Ocean is classified as the main source of moisture to southern Africa rainfall, with the South Indian anticyclone (Mascarene) playing a huge role of moisture advection into the land regions of southern Africa (Blamey, 2012; Driver, 2014). Atmospheric circulation patterns are influenced by the anomalous SST conditions within the Indian Ocean basin, which play a significant role in enhancing or weakening of the moisture advection to the interior of the subcontinent (Blamey, 2012). Rouault et al. (2003) highlighted that the occurrence of strong warm events in the tropical South East Atlantic Ocean during the late summer can amplify local atmospheric instability, evaporation and rainfall. During these warm events, increased low-level moisture coming from tropical South East Atlantic Ocean acts to increase the coastal Angolan rainfall and wetter conditions in northern Namibia (Reason, 2015). The regional atmospheric circulation of southern Africa is not only strongly influenced by the neighboring oceans, but it has been found to be sensitive to SST variability in the Pacific Ocean through a phenomenon called ENSO which will be explored in detail in the next subsection.

2.4.1. Subtropical Indian Ocean Dipole

At a regional scale, SST variations in the Indian Ocean are known to influence the inter-annual rainfall fluctuations over South Africa (Reason, 2001). The major climate mode in the Indian Ocean controlling the SST anomalies is called Subtropical Indian Ocean Dipole (SIOD) and was found by Behera and Yamagata (2001) using simple Empirical Orthogonal Function (EOF) extracted from SST observational data. The authors highlighted that the SIOD is significant at the inter-annual scale during austral summer, and this climatic mode oscillates between two phases: positive and negative phases (Reason, 2001; Hermes and Reason, 2005). The positive phase is characterised by positive SST anomalies at the south-western side of the Indian Ocean and negative SST anomalies at the south-east (Australian side), while the reverse occurs during a negative phase (Behera and Yamagata, 2001; Reason, 2001). The positive phase of the SIOD influences the positive anomalous rainfall over many regions in south-central Africa, while the negative phase leads to negative anomalous rainfall (Behera and Yamagata, 2001). Reason (2001, 2002) further highlighted that during the negative phase of the SIOD, decreased precipitation is observed over the south-eastern part of South Africa influenced by low-level divergence. Furthermore, the decreased evaporation over the cold pole at the south-west Indian Ocean during a negative phase leads to less moisture advection towards Mozambique and south-eastern Africa (Reason, 2001). The negative moisture advection is influenced by a high-pressure anomaly produced above the colder SIOD pole side which weakens the onshore flow to Mozambique and hinterlands. When the signs reverse, the opposite happens.

2.4.2. El Niño Southern Oscillation and southern African Rainfall.

ENSO is a naturally occurring phenomenon involving ocean-atmosphere interactions which lead to fluctuations in ocean temperatures in the central and equatorial Pacific Ocean. The term “El Niño” was coined by fishermen from Ecuador and Peru, to refer to the annual warming of water during Christmas time at the coast. Currently, the term in the climate science community refers to anomalous warming of the central and eastern Pacific Ocean. Consequently, El Niño (warm phase) is characterised by warmer than normal SST over the Pacific Ocean and the opposite occurs during the La Niña event (cool phase). The atmospheric component of ENSO, Southern Oscillation (SO) refers to the fluctuation (in a see-saw manner) of atmospheric mass between the eastern and western Pacific Ocean (Cane, 2005). This mode can further be measured by using Southern Oscillation Index (SOI), an index that defines normalised Sea Level Pressure (SLP) difference between Darwin and Tahiti. The positive

phase of SO is indicated by above normal SLP at Tahiti and below normal SLP at Darwin. The reverse occurs during the negative phase of the SO. The prolonged period of the positive phase of the SO is associated with La Niña, while the negative phase is associated with El Niño event. During these ENSO episodes: temperature, SLP and wind field changes occur in the Pacific Ocean, creating different weather and climatic conditions during La Niña and El Niño over southern Africa and across the globe (Tyson and Preston-White, 2000). For instance, during El Niño episodes, the SST and SLP increases in the Pacific Ocean, leading to a deeper thermocline and weaker winds, while the reverse occurs during La Niña. Consequently, the changes in the mentioned above variables affect the location of the major cloud bands which applies modifying effects to the rainfall of the continents.

At a spatial scale, ENSO is known to influence SST in the Indian, Atlantic Ocean and South Africa west coast upwelling system (Dufois and Rouault, 2012). It is the main driver of the inter-annual rainfall variability in southern Africa although its influence shows regional variations for each ENSO event. The effect of ENSO is at maximum during summer of December to March and its influence is strongest in the south-eastern part of the subcontinent (Richard et al, 2001). During El Niño events, there is anomalous lower level divergence over the landmass preventing maritime moisture transport to southern Africa, due to the changes in the Walker and Hadley circulation (Abiodun and Meque, 2014) leading to the reduction in seasonal rainfall (Dieppois et al., 2015). During La Niña summer episode, enhancement of precipitation is caused by the dominance of anomalous low- level divergence over southern Africa (Abiodun and Meque, 2014). Over the Atlantic Ocean, El Niño produces an equatorward shift in the SAA and westerly winds to the south leading to a weakening of upwelling favorable conditions over the west coast of South Africa (Dufois and Rouault, 2012). The weak upwelling during this event is induced by a reduced south- easterly wind which promotes cold SST anomaly along the west coast of southern Africa (Dufois and Rouault, 2012). During La Niña event the opposite occurs, the south-easterly is stronger and upwelling is more intense and the coastal waters are colder. Reason et al,(2006) demonstrated that ENSO also influences the SICZ, a predominant summer feature that acts to transport moisture and energy to higher latitudes and influences the jet streams and the generation of the mid-latitudes depression which have a significant impact on the development of the main summer synoptic features of southern Africa. Since the 1970s, El Niño (La Niña) has been documented to favour droughts (wet seasons) around southern Africa (Richard et al., 2001; Philippon et al., 2012; Dieppois et al., 2015). During the relatively weak El Niño of 1991/1992 and 2002/2003, widespread and severe summer droughts occurred over a large area around southern Africa (Reason and Jagadheesha. 2004; Rouault and Richard 2003, 2005; Fauchereau et al., 2009): the northern part of southern Africa, Zimbabwe and Namibia (Fauchereau et al., 2009). However, during the strongest El Niño of 1997/ 1998, whilst extreme climate anomalies occurred all over the globe, South Africa was an exception as it received near average precipitation amounts for the season despite a dry start to the summer rainy season (Tyson and Preston-White, 2000; Richard et al., 2001 Rouault and Richard 2003). Reason et al. (2006) proposed that this could have been due to warm SST anomalies encountered in the south-east Atlantic and that the Angola Low was not significantly weakened during this period, therefore there was advection of moister tropical marine air in the Angola Low. This served as a source region for the development of the cloud bands during 1997/8 El Niño summer. This demonstrates how ENSO is not systematically correlated to the dry conditions over southern Africa (Fauchereau et al., 2009). Mason and Goddard (2001) further highlighted that a high frequency of above normal precipitation during a very strong El Niño conditions doesn't assure a high frequency of below normal rainfall.

Probably because of internal variability and because inter-annual variability in southern African precipitation responds to the SST anomalies over the surrounding Indian and South Atlantic (Fauchereau et al., 2009 and Richard et al., 2001) which may not be linked to ENSO. During non-ENSO dry years, the warm anomalies in the eastern equatorial Indian Ocean are frequently associated with dry conditions over southern Africa (Richard et al., 2001). Over northern South Africa, non-ENSO droughts show a strong relationship with the cold, dry air advected over South Africa from the South Atlantic, due to a cyclonic anomaly located over southern Africa (Reason et al., 2006).

2.5. Droughts

Southern Africa is susceptible to droughts due to its high inter-annual rainfall variability. The mere fact that this subcontinent's economy depends on rain-fed agriculture, makes it more vulnerable to drought. Drought is one natural hazard with a complex nature in both temporal and spatial scales and is often difficult to monitor (Manatsa et al., 2010; Ujeneza and Abiodun, 2015). Hence, to date, there is no universal definition of the term drought. This is so, because droughts have different meanings to different sectors due to different time scales, intensity, place of occurrence, frequency and time of occurrence (Rouault and Richard; 2003 Manatsa et al., 2010; Malherbe et al., 2016). For example, farmers are more interested in how the droughts affect the crop production while the hydrologists are more concerned on how the hydrological system will suffer during drought occurrence. Accordingly, droughts have been classified into four different categories: agricultural, meteorological, socio-economic and hydrological droughts. An agricultural drought can be defined as a situation whereby there is no sufficient moisture to support crop production (Manatsa et al., 2010). The time scale for an agricultural drought to occur is a season, which is 3-6 months (Rouault and Richard, 2003). A meteorological drought can occur from a month to years and is distinguished by negative anomalous rainfall, which is influenced by large scale atmospheric modes (e.g. ENSO and SIOD), and acts as a precursor to other different kinds of droughts (Dai, 2011). A hydrological drought is characterised by rainfall shortages over a long period of time (12-24 months or more) and it is manifested on surface water supply (Rouault and Richard, 2003). And, lastly the socio- economic drought is characterised by economical shortage of water and serves to address the effects of all the different types mentioned above (Peters, 2003).

2.5.1. Drought Monitoring and Index

A drought index becomes handy when quantifying and monitoring droughts as it can provide a simple, clear and quantitative assessment (Manatsa et al., 2010) of the main properties of the droughts (time, duration, frequency and occurrence). The Palmer Drought Severity Index was one of the widely used drought indices developed in the USA to monitor droughts but, due to some limitations it couldn't be able used as an analysis method that addresses the main properties of a drought mentioned above. However, the Standard Precipitation Index (SPI) was approved and proposed by the World Meteorological Organisation (WMO) as the standard drought index and has been developed by Mckee et al. (1993), to measure rainfall anomalies and making drought monitoring simpler and at the same time ignoring other hydro-meteorological variables such as temperature and soil moisture (Manatsa et al., 2010). The main advantage of the SPI is its ability to do simple calculation, and its ability to detect the drought onset, temporal succession and spatial extension (Rouault and Richard 2003, 2005). The other advantage of the SPI is manifested by its ability to monitor wet and dry episodes over a wide classification of temporal scales (Manatsa et al., 2010; Mckee et al., 1993; Malherbe et al., 2016). The application of SPI has been of importance to southern Africa because of its capability to consistently deal with the high inter-annual rainfall variability that is influenced by the orography, the contrasting oceans and geographical position (Rouault and Richard, 2003). Thus, it has been previously used to study droughts over the subcontinent; for instance, Rouault and Richard (2003, 2005) utilised the SPI to study the intensity and spatial extent of drought in South Africa, while Lyon (2009) utilised the SPI to assess the southern Africa droughts and heat waves through observations and coupled models. Furthermore, Manatsa et al. (2010) utilised the SPI to study the agricultural droughts in Zimbabwe, Ujeneza and Abiodun (2015) simulated the relationship between summer droughts and ENSO in southern Africa using regional climate models. Finally, Malherbe et al. (2016) used the index to examine the South African droughts and decadal variability.

3. Data and Methods.

3.1. Atmospheric circulations

To understand the atmospheric and oceanic influence on southern African summer rainfall, monthly Optimum Interpolation (OI) Reynolds SST dataset was used (Reynolds SST; Reynolds et al., 2002). The Reynolds SST (OI SST) data is found at 1º×1º regular grid from January 1982 to present. The dataset is derived from daily merged, in situ, high resolution (9 km) infrared satellite observations from the AVHRR (Advanced Very High-Resolution Radiometer) instrument on board NOAA (National Oceanic and Atmospheric Administrative). Rouault et al. (2010) emphasized that the Reynolds SST can be used to study the impact of ENSO on coastal zone of South Africa.

For global rainfall monthly Global Precipitation Climatology Centre (GPCP, Huffmann et al., 2013) Version 2.2 was used. The monthly precipitation dataset is from January 1979 to present. The dataset combines the satellite and observation data into 2.5 º × 2.5 º global regular grid.

The National Centre for Environmental Prediction (NCEP) Reanalysis dataset are used in this study to assess circulation changes associated with El Niño related droughts. The monthly NCEP dataset utilised has a time resolution and spatial resolution of 2.5 º × 2.5 º. It should be noted that the spatial resolution of the NCEP reanalysis data does not properly solve upwelling regions (Rouault et al., 2010) and topographic details well (Mulenga et al., 2003). However, for analysing the large-scale circulation anomalies over the South Atlantic to South Indian Ocean Region, NCEP resolution is adequate. In this study: geopotential height (m) at 1000 hPa and 500 hPa levels were considered.

The composite atmospheric and oceanic anomalous conditions during El Niño years from December 1983 to March 2016, summer 2014/2015 and summer 2015/2016 was constructed using the NOAA Earth Research Laboratories Physical Sciences Division website found online at: www.esrl.noaa.gov/psd/ . The composites are calculated by averaging summer seasons during the El Niño events from 1982 to 2016. The anomalies are the deviation from the summer mean climatology and are calculated by subtracting any quantity from the mean climatology.

3.2. Nino 3.4 Index

To calculate the El Niño Index over the Pacific Ocean, SST was extracted between ([5º N-5 º S, 120 º - 170 º W]) in the Nino 3.4 domain using the Extended Reconstructed Sea Surface Temperature (ERSST) v4 that is obtained online from Earth System Research Laboratory (ESRL) at NOAA (http://www.esrl.noaa.gov/data/gridded/data.noaa.ersst.html). The data is on a 2º x 2 º regular grid and extends from 1854 until present. To compute the Nino 3.4 index, averaged summer SST (December, January and February, DJF) were extracted from SST from the defined region above and further standardized over the climatological period from 1921 to 2016.

3.3. SPI data

The study used monthly precipitation provided by the South African Weather Service (SAWS) from January 1921 to December 2016 to calculate the SPI. The SAWS categorises the country into the 94 rainfall districts (Figure 1), of which each rainfall district at least combines the mean of 5 to 15 rain gauges (Rouault and Richard, 2003). The 94 districts are further

subdivided into 8 homogenous rainfall areas (Figure1), since rainfall is a complex event that is highly variable in space and time. Therefore, identification of homogenous rainfall regions is very critical as it aids one in analyzing the intensity, extent and patterns of rainfall by resolving smaller scale variations (Awan et al., 2015). A variety of techniques are applied to identify homogenous rainfall such as cluster analysis, correlation analysis and Principal Component analysis, and further details on how cluster analysis was applied to defined homogenous rainfall regions can be found at Mimmack et al. (2001).

This study will only calculate the SPI for austral summer rainfall regions (region 4- 8) from 1921 to 2016.The SPI were considered for 3-time scales: 3 month duration till the end of February for the heart of the summer rainfall season, 5 months duration until the end of March for all summer seasons and 17 months duration till the end of March for a nearly two year long summer season index. Further details on how to compute the SPI can be obtained from Hayes et al. (1999). The SPI program only requires rainfall data in ASCII format and was downloaded from http://drought.unl.edu/MonitoringTools/DownloadableSPIProgram.aspx).

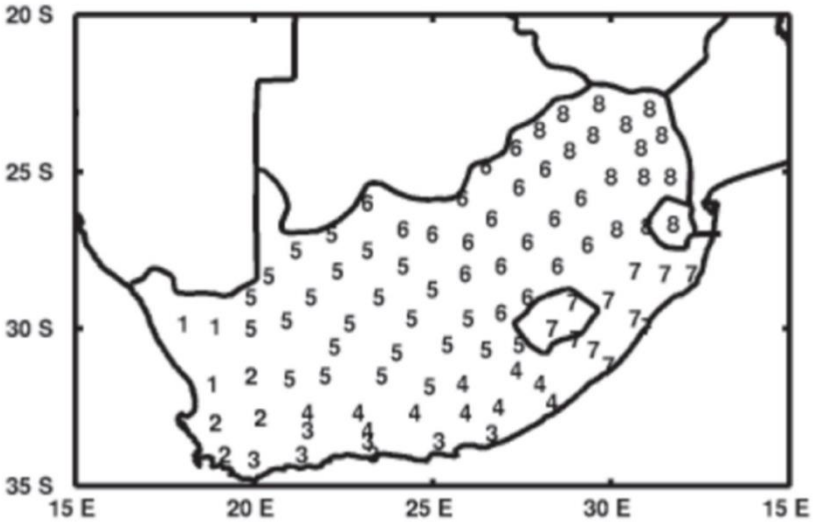

Figure 1: Location of the 94 rainfall districts of the SAWS. The 94 districts are further categorised into 8 homogenous rainfall area defined by SAWS, namely: North-Western Cape (1), South-Western Cape (2), South Coast (3), Southern Interior (4), Western Interior (5), Central Interior (6), Kwa-Zulu Natal (7) and North-Eastern Interior (8). (Rouault and Richard 2003).

4. Results and Discussion

4.1. Rainfall over southern Africa

To investigate the impact of ENSO on rainfall, composite maps of mean and anomalous rainfall during austral summer were constructed. Figure 2 shows the global summer rainfall composite (averages) anomaly during El Niño also called canonical El Niño conditions. It is established by

calculating the mean condition during several El Niño events and subtracting the climatology for the corresponding period, this applies also to SST and geopotential height anomalies. El Niño summer years considered were 1983, 1987, 1992, 1995, 1998, 2002, 2005, 2007, 2010, 2015 and 2016. Note that those events started the year before and El Niño usually matures in austral summer. For instance, 1983 corresponds to the 1982/1983 El Niño during its mature phase. In summary, Figure 2 shows the average impact in mm/day one can expect during an El Niño event, but it should be highlighted that different impacts can be expected during an individual year. During El Niño event, wetter than normal conditions are observed over central and eastern Pacific Ocean, eastern part of South America, central Indian Ocean, northern Madagascar and the eastern side of South America (Paraguay, eastern Argentina and southern Paraguay). While, during the same event, drier than normal are observed over southern Africa, north-eastern part of South America, northern Australia and maritime continent (Philippines, Malaysia, Papua New Guinea).

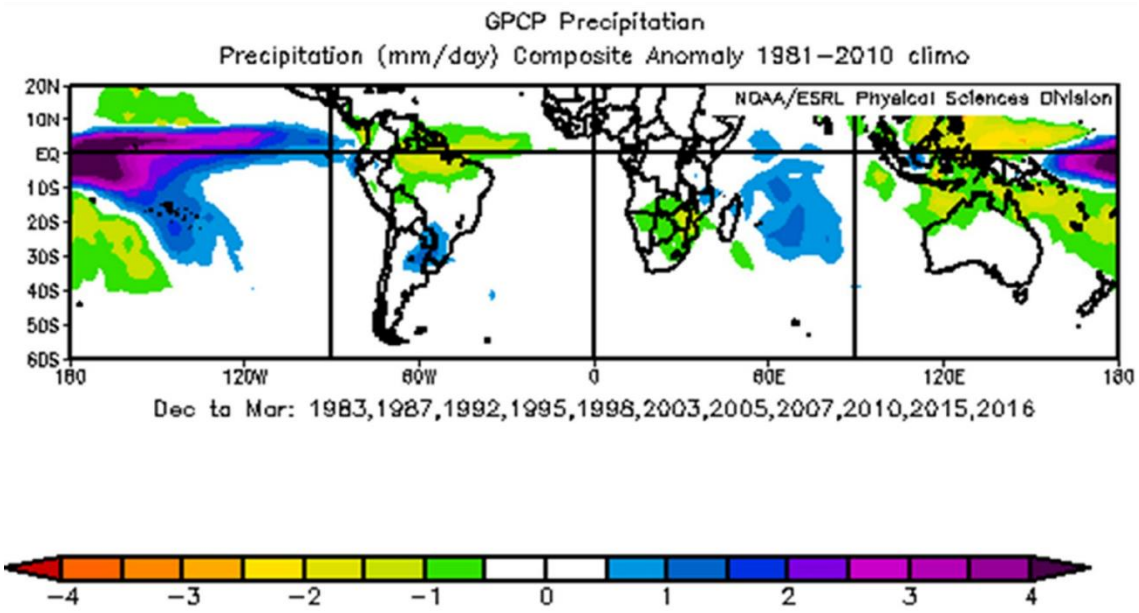

Figure 2 : Global rainfall (mm/ day) El Niño composite anomaly from climatology from December 1982 to March 2016 using GPCP data. A positive (negative) anomaly implies wetter (drier) than normal rainfall. El Niño years considered were 1983, 1987, 1992, 1995,1998, 2002, 2005, 2007 ,2010, 2015 and 2016.

Figure 3a (top left) is the same as Figure 2 but zoomed over southern Africa, and Figure 3b (top right) and c (bottom) show the summer season of summer 2014/ 2015 and 2015/2016, respectively. During the summer of 2014/2015 wetter than normal rainfall is found over eastern Mozambique and southern Madagascar while drier than normal rainfall is over the subcontinent, with stronger anomalies than expected found over Zambia, north part of South Africa and Mozambique. Figure 3c displays similar patterns to Figure 3b but with stronger negative rainfall anomalies moving towards the east and covering Madagascar, while the normal rainfall is experienced in central Botswana and Namibia. There are similarities and differences between El Niño composite anomalies, summer 2014/2015 anomalies and summer 2015/2016 anomalies. To better understand those differences, individual months for the two summer seasons will be discussed below.

Individual months within the summer seasons of 2014/2015 (Figure 4) and 2015/2016 (Figure 5) are considered to understand the contributions they had on the negative rainfall anomalies and to get more insights into the deviation from the canonical El Niño event. A canonical El Niño is a standard or typical El Niño to which other events are compared. In December 2014, north-east

South Africa, Botswana, Zimbabwe and Mozambique received more rainfall than normal compared to the other countries of the subcontinent (Figure 4a).

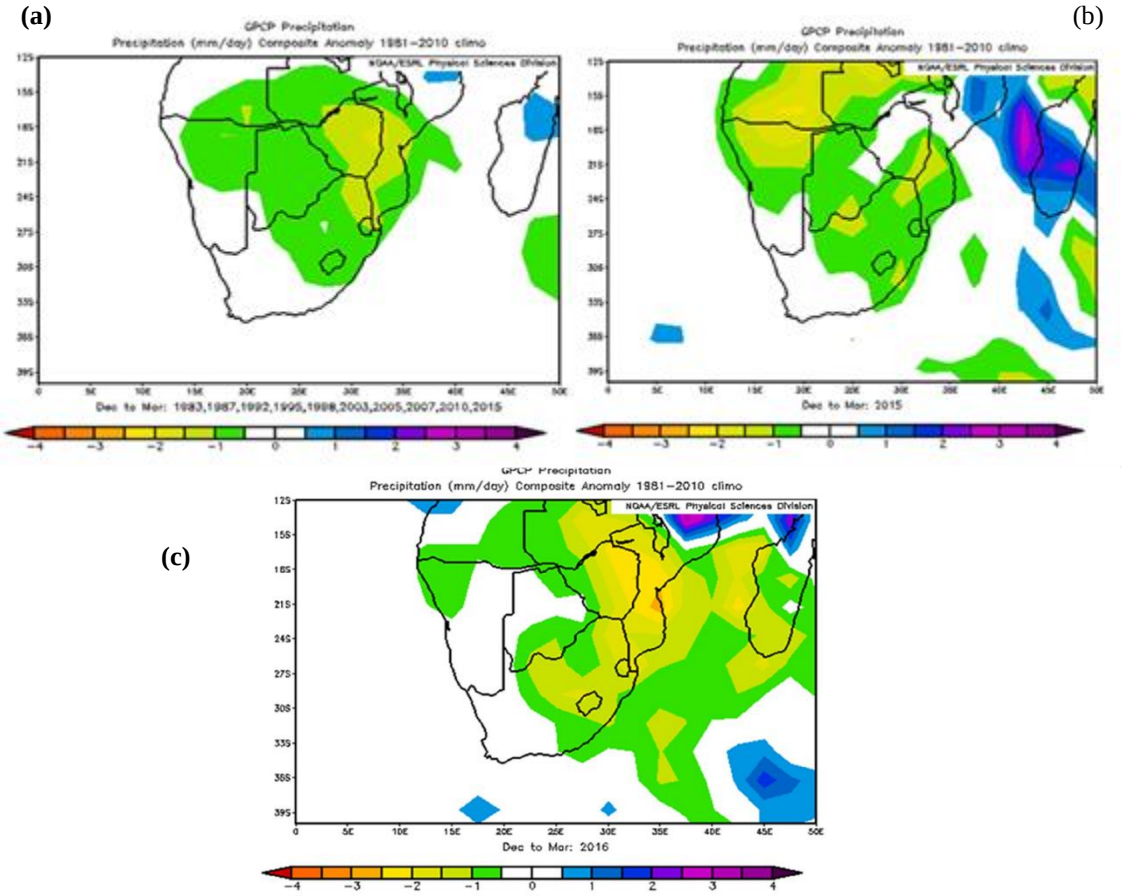

Figure 3 : Top left El Niño composite of rainfall anomalies (mm/day) from Dec1983 to Mar 2016 for Southern Africa. Top right: same for 2014/2015 summer and, bottom: 2015/2016 summer (c). Positive anomalies mean wetter than normal rainfall and negative anomalies mean drier than normal rainfall.

During January 2015, it is notable that wetter than normal conditions occurred in central Angola, Northern Mozambique, Malawi and Madagascar (Figure 4b). However, South Africa, Namibia and Botswana were drier than normal and west coast of South Africa while southern Namibia received normal rainfall. February 2015 (Figure 4c) was the driest month over southern Africa except over Mozambique and eastern Madagascar. During March 2015, drier than normal conditions occurred over Malawi, Zimbabwe, Mozambique and the northern part of South Africa (Figure 4d) while normal rainfall occurred over most central South Africa, Namibia and Botswana.

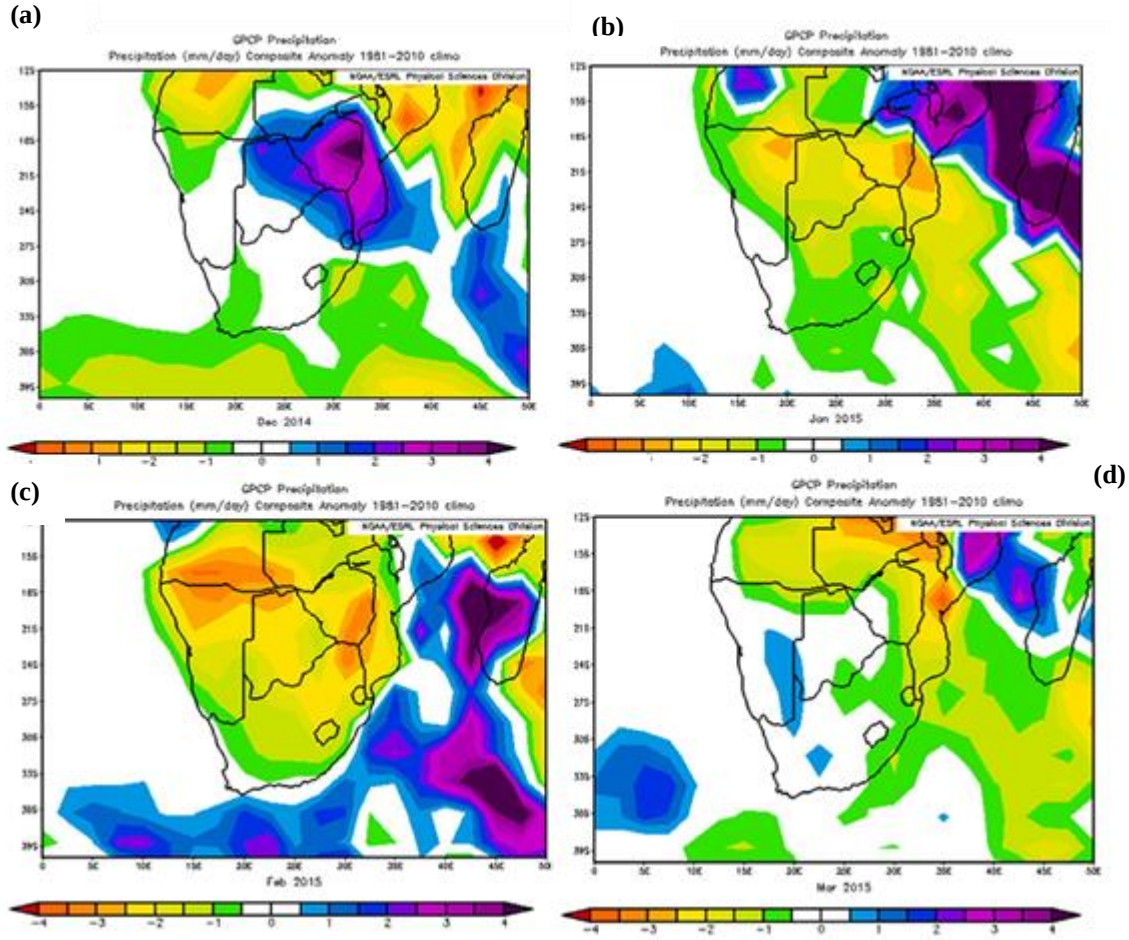

Figure 4: From top to bottom and left to right: rainfall anomalies (mm/day) from climatology over Southern Africa during the summer season 2014/2015 (a) December 2014 (b) January 2015 (c) February2015 and (d) March 2015. Positive (negative) anomalies indicate wetter (drier) than normal rainfall.

Unlike December 2015 (Figure 4a), Figure 5a shows drier than normal rainfall over the subcontinent except over western Angola and Northern Mozambique. January 2016 (Figure 5b) presents similar results to January of 2015, the only differences are observed over south-western South Africa and south of Namibia with above normal rainfall experienced over these two regions while central Namibia experienced normal rainfall. February 2016 displays similar patterns as February 2015, but with more intensified negative anomalies (<-4 mm/day) over Mozambique. During March 2016 (Figure 5d) rainfall conditions around southern Africa are becoming normal, but the north-eastern part of South Africa experienced wetter than normal rainfall, which is very different compared to March 2015. Analysing from these results, we can deduce that the stronger negative anomalies observed over the summer of 2015/2016 as compared to the 2014/2015, were rather influenced by stronger below normal patterns observed during January and February 2016.

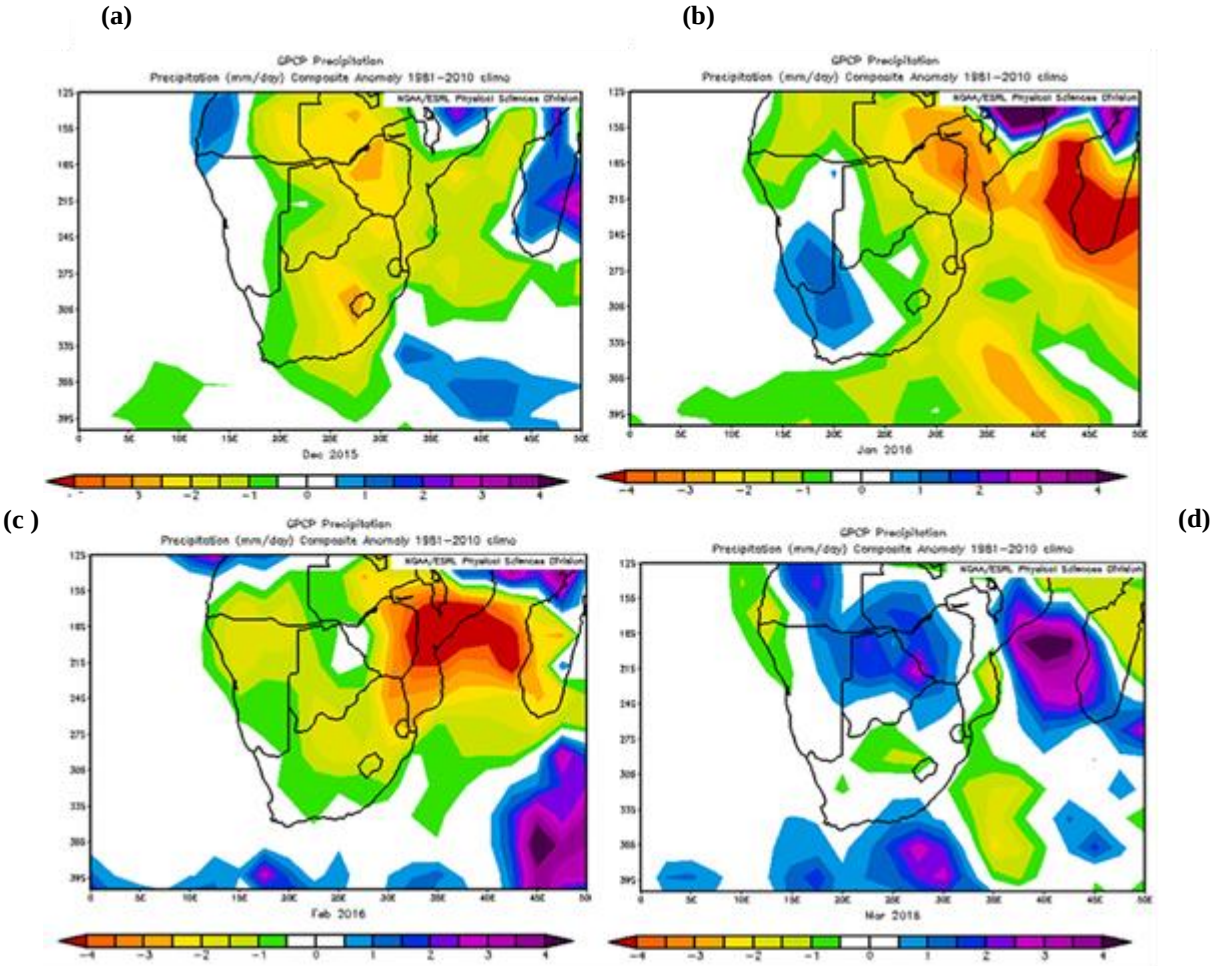

Figure 5: From top to bottom and left to right: rainfall anomalies (mm/day) from climatology over Southern African during the summer season 2015/2016 (a) December 2015 (b) January 2016 (c) February 2016 and (d) March 2016. Positive (negative) anomalies indicate wetter (drier) than normal rainfall.

4.2. Sea Surface Temperature

Figure 6 shows the canonical spatial pattern of El Niño impact on global SST. It is a composite anomaly from a mean of summer conditions that occurred during El Niño seasons defined above. El Niño summer season years considered were 1983, 1987, 1992, 1995, 1998, 2002, 2005, 2007, 2010, 2015 and 2016. Warmer than normal SST anomalies are found in the eastern and central equatorial Pacific, Indian and South Atlantic Oceans and colder than normal SST are found in the southern Pacific and southern Atlantic Ocean (South of 34º S). Zooming over southern Africa during El Niño years (Figure 7a), warmer than normal SST anomalies are found over the Southwest Indian Ocean (SWIO), Southeast Atlantic Ocean and along the west coast of South Africa. However, cooler than normal SST are found over the Namibia coast [17 º- 26º S]. Figure 7b shows the summer 2014/2015 SST anomalies over southern Africa, evident is the abnormal negative SST anomaly over southern Africa coast, SWIO, Mozambique Channel as well as over the subtropical Atlantic (~ 33°- 40° S; 0°-15°E). Positive SST anomalies are found over the South Atlantic Ocean; however, the amplitude of SST anomaly is higher during summer 2014/2015 than during the El Niño years.

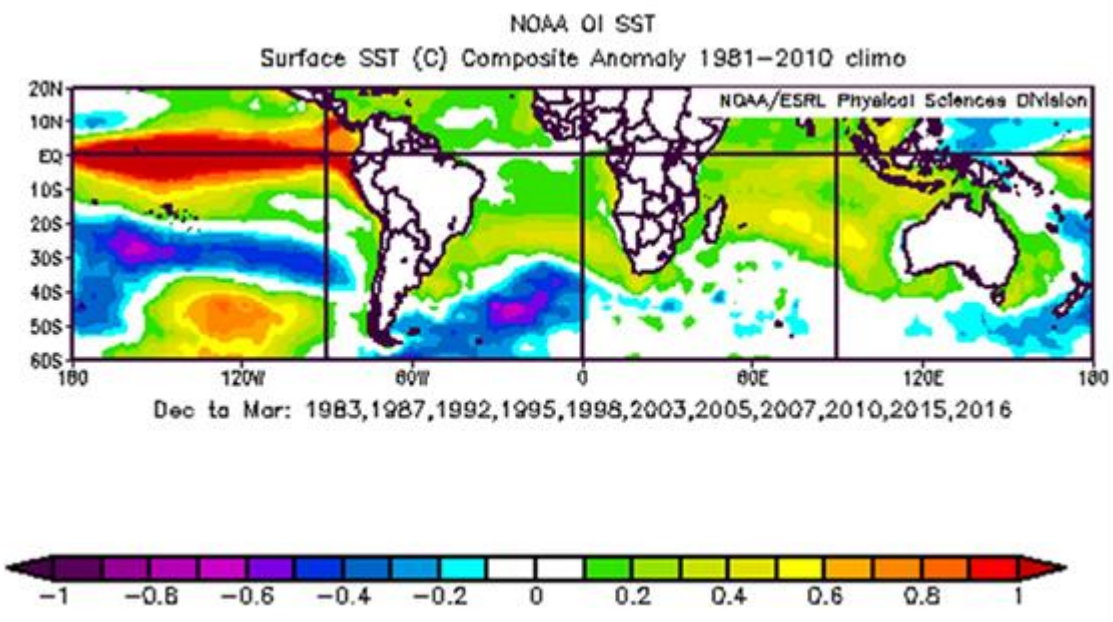

Figure 6: Global SST (^{0}C) composite anomaly from climatology for the summer season from December 1982 to March 2016) using NOAA OI SST data during El Niño years. Positive (negative) anomalies indicate warmer (colder) than normal SST. El Niño years considered were 1983, 1987, 1992, 1995, 1998, 2002, 2005, 2007, 2010, 2015 and 2016

The difference between the summer 2014/2015 (Figure 7b) SST anomalies and the canonical El Niño summer over southern Africa are the colder than normal SST over Madagascar Channel, south coast and west coast of South Africa. However, the warmer than normal SST over the south Atlantic and Pacific Ocean are similar to canonical El Niño summer over the region. Unlike summer 2014/2015, the summer of 2015/2016 (Figure 7c), experienced warmer than normal SST across the entire south Pacific and Indian ocean, except for a smaller domain over the south Indian ocean.

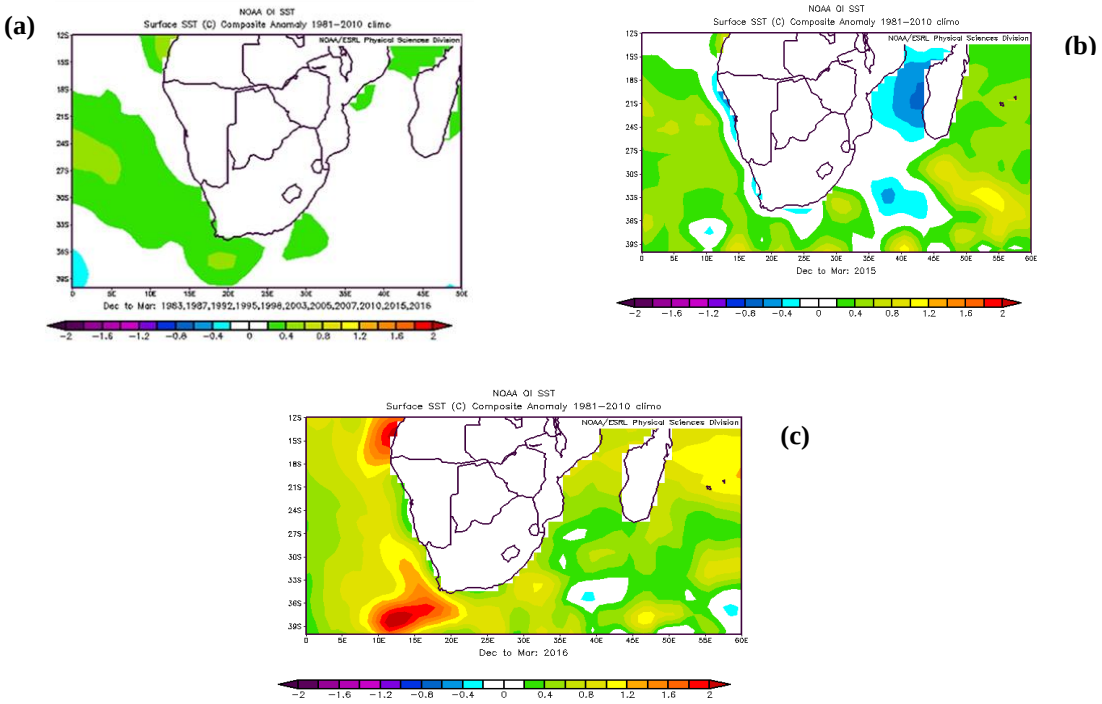

Figure 7 : Composite of SST anomalies (^{0} C) during El Niño for the summer season from Dec 1983 to Mar 2016 for southern Africa (a, top left), (b, top right) 2014/2015 and 2015/2016 (c, bottom). Positive anomalies means warmer than normal SST and negative anomalies mean colder than normal SST.

Furthermore, SST anomalies are plotted for each month for the summer 2014/2015 in Figure 8 to understand the origin of the difference from canonical El Niño pattern and possible regional impacts on the rainfall. In December 2014 (Figure 8a), warmer than normal SST in the South Atlantic Ocean and over the Angolan coast are similar to the canonical El Niño pattern over southern Africa. Cooler than normal SST are found over south Indian Ocean, Madagascar, south coast and Namibian coast which are different from the canonical El Niño pattern. Colder SSTs over the west coast are different from canonical El Niño. During January 2015 (Figure 8b), south Indian Ocean and south Atlantic Ocean mimics the canonical El Niño pattern over the subcontinent but with stronger warm SST anomaly.

The warming at the Namibian coast and the Mozambique Channel differentiate this month from canonical El Niño pattern. Dieppois et al. (2015) suggested that the warming at the subtropical Atlantic Ocean could be due to southerly migration of the SAA, the shift could have decreased the wind off the Namibia coast leading to suppressed upwelling. During February (Figure 8c), there is warmer SST anomaly from the west at the SWIO and weaker positive SST anomaly over south Atlantic Ocean when compared to January 2015 SST anomaly. The cooling over the Namibian coast and warming over the South Atlantic during this month is the canonical El Niño pattern. However, the cooling over the Angolan coast, Port Elizabeth coast, east coast of South Africa and Mozambique Channel are not expected during El Niño.

Lastly during March 2015 (Figure 8d), warmer SST over the Angolan coast, south Atlantic and south Indian Ocean are similar to canonical El Niño pattern. However, Mozambique Channel is different when compared to canonical El Niño pattern over the area. The cooler SST along the Benguela Current system throughout December 2014 and January 2015 and Madagascar Channel could have led to the seasonal cooling along the entire southern African coast and the Mozambique Channel evident on Figure 7b.

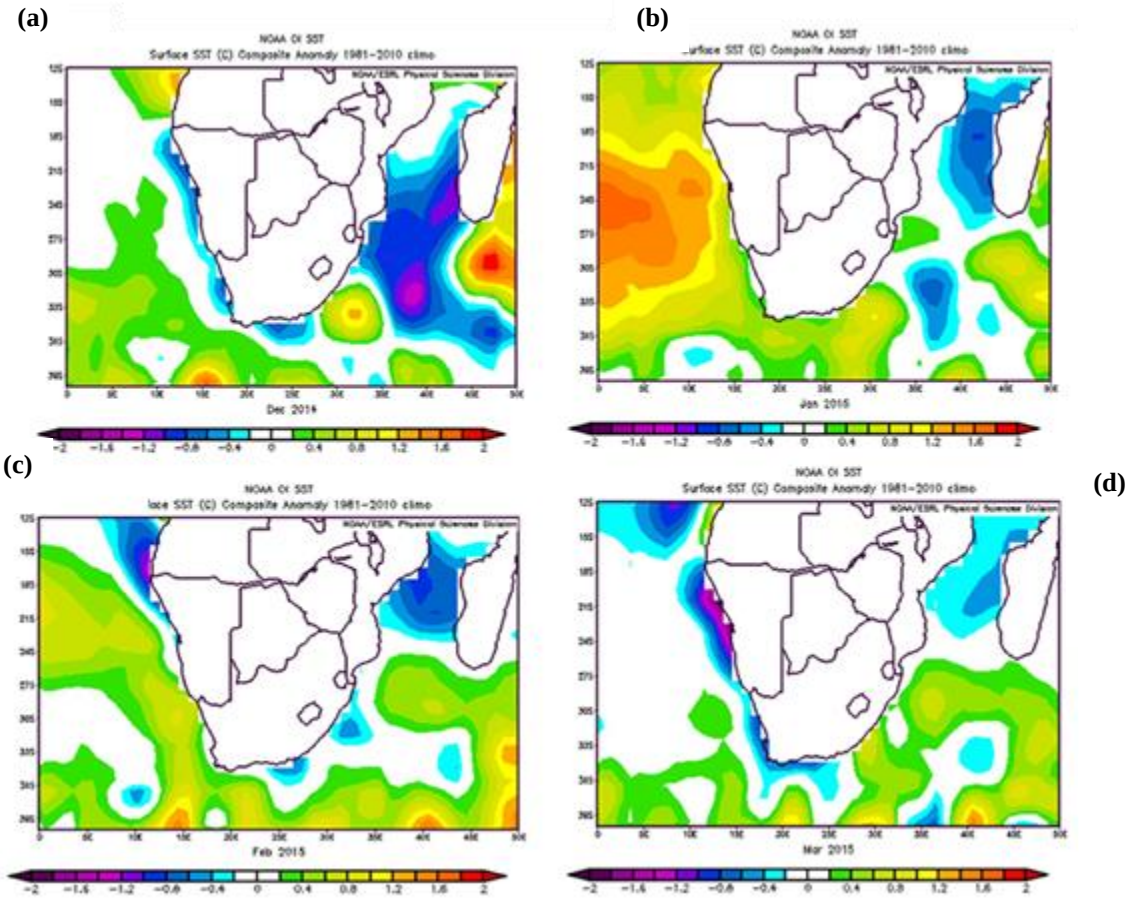

Figure 8: SST anomalies (^{0} C) from climatology over southern African during the summer season 2014/2015. (a) December 2014 (b) January 2015 (c) February 2015 and (d) March 2015. Positive (negative) anomalies indicate warmer (colder) than normal SST.

In comparison, December 2015 (Figure 9a) and January 2016 (Figure 9b) mimics the SST patterns observed over its summer average (2015/2016). During February 2016 (Figure 9c), there is colder SST extending from the Indian Ocean with the south coast having colder than normal SST. March 2016 (Figure 9d), shows similar patterns with a canonical El Niño, the only exception is observed over the west coast of South Africa, which is characterised by colder than normal SSTs.

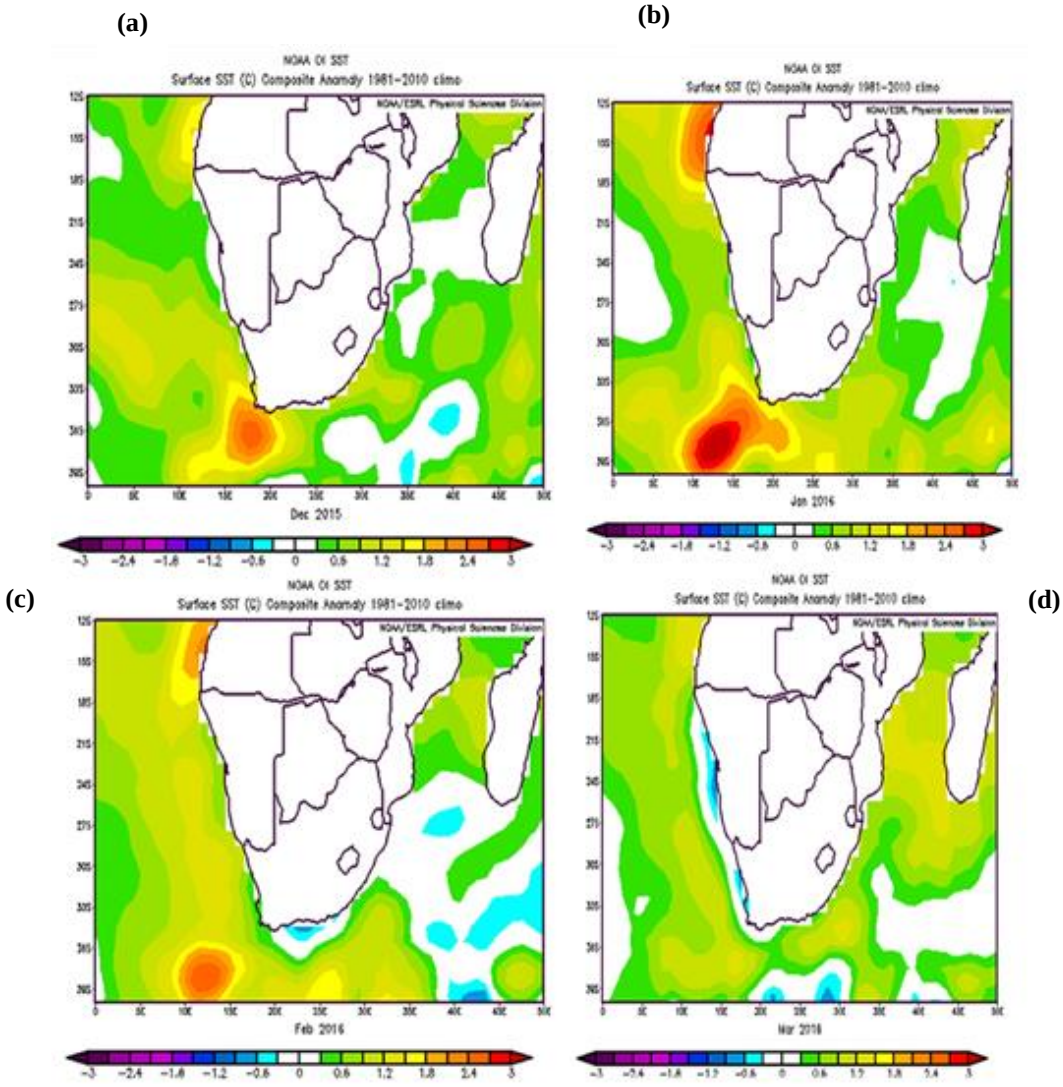

Figure 9: SST anomalies (^{0}C) from climatology over southern African during the summer season 2015/2016. (a) December 2015 (b) January 2016 (c) February 2016 and (d) March 2016. Positive (negative) anomalies indicate warmer (colder) than normal SST.

4.3. Geopotential height at 1000 hPa

Figure 10 shows the composite anomaly from the climatology during El Niño events over southern Africa for sea level pressure (1000 hPa). At the surface (~1000 hPa) higher than normal pressure anomalies are evident over Australia, Africa, South Pacific and the Indian Ocean. In general, high pressure prevents rain from occurring by preventing air masses from the surface to rise. In that respect, it is interesting to note that no surface pressure anomalies are found in the middle of the subcontinent (southern Africa) during ENSO which would be associated with normal rainfall which is clearly not the case. This is probably because higher than normal surface temperature can enhance vertical velocity which can overcome the general high-pressure anomalies found at higher level of the troposphere during ENSO such as the 500 hPa which is shown in Figure 14 and other tropospheric levels (not shown). So, the surface conditions are not enough to overcome pressure anomalies created in the troposphere by the teleconnection with Pacific and Indian Oceans and to generate normal rainfall.

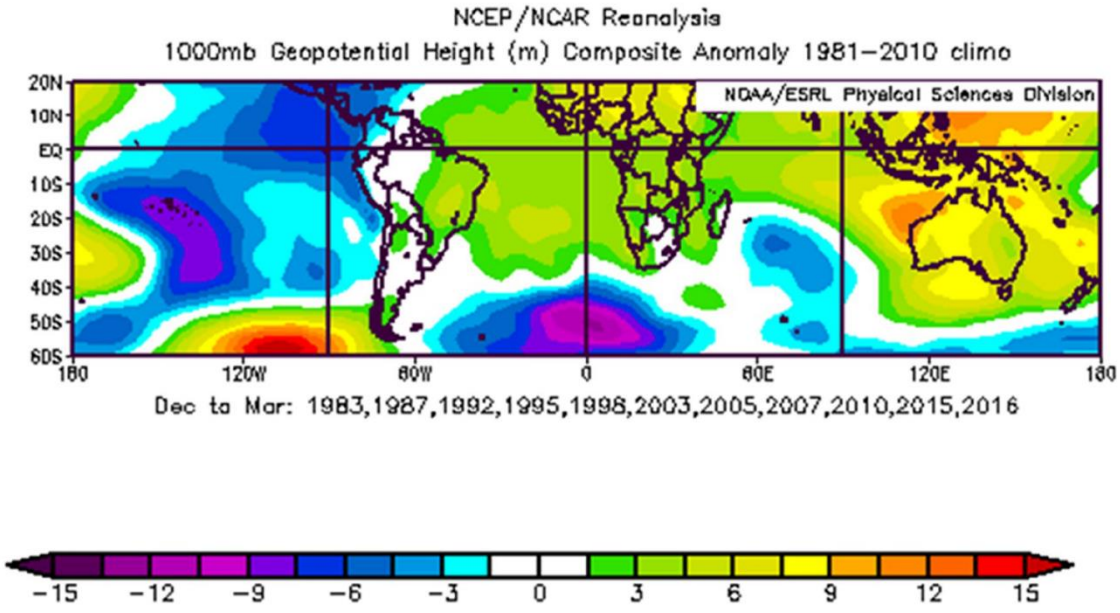

Figure 10: Composite for geopotential height anomaly (m) for the summer season during El Niño years from December 1982 to March 2016 at 1000 hPa. Positive anomalies indicate higher than normal pressure and negative anomalies indicate lower than normal pressure. El Niño years considered were 1983, 1987, 1992, 1995, 1998, 2002, 2005, 2007, 2010, 2015.

Figure 11a shows geopotential height anomaly over southern Africa during El Niño summer while Figure 11b show the geopotential height anomalies the subcontinent during the summer 2014/2015. Higher than normal pressures cover southern Africa, lower than normal pressures are over the South Atlantic Ocean and normal pressure occur over central South Africa and Botswana during a canonical El Niño summer. The summer season 2014/2015 mimicked the canonical El Niño pattern with higher than normal pressures over the interior. However, the lower than

normal pressures over Madagascar, South East Indian Ocean, central Botswana and South Africa are different when compared to Figure 11a.

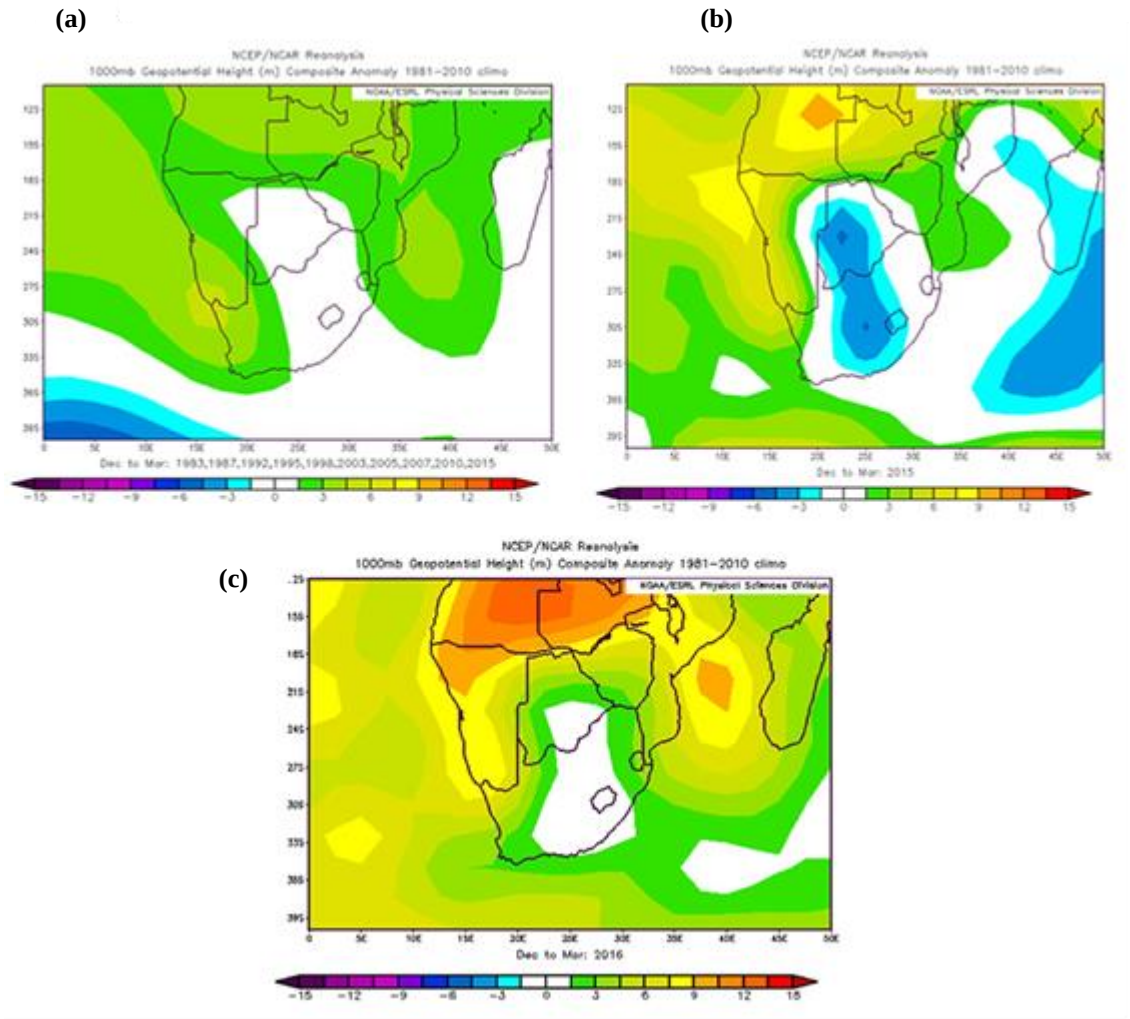

Figure 11: Top left: composite of 1000 hPa geopotential height anomaly (m) during El Niño for the summer season Dec 1982 to Mar 2016 for southern African (a), Top right 2014/2015 (b) and bottom 2015/2016 (c). Positive anomalies mean higher than normal pressure and negative anomalies mean lower than normal pressure.

It is also evident that intensified anomalous high pressure is over northern Angola and western Namibia during the summer 2014/2015. Figure 1 1 c shows the geopotential anomalies during the summer of 2015/2016 over the subcontinent. The pressure patterns during this summer mimic the canonical El Niño pattern but with higher magnitude. The only difference between this summer and the canonical summer event is the higher than normal pressure at South Atlantic Ocean.

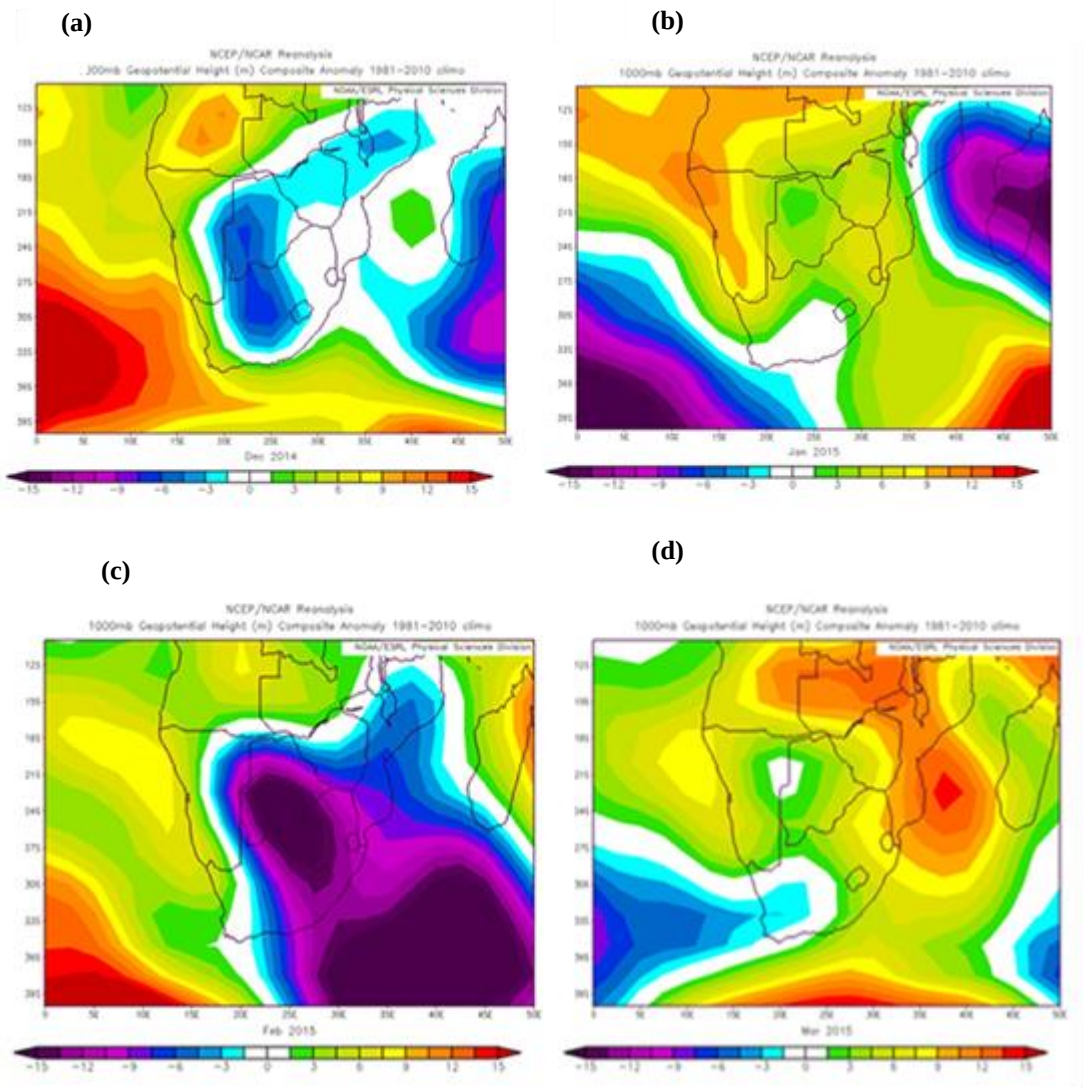

Figure 12 : 1000 hPa geopotential height anomalies (m) during summer season (December 2014-March 2015) over Southern Africa at 1000 hPa. (a) December 2014, (b) January 2015, (c) February 2015 and (d) March 2015. Positive anomalies mean higher than normal pressure and negative anomalies mean lower than normal pressure.

Figure 12a show geopotential height anomalies during individual months within the summer season of 2014/2015 over South Africa. The higher than normal geopotential height anomalies during December 2014 are found over the South Atlantic Ocean and Angola and are canonical of El Niño conditions over southern Africa. However, the anomalous low pressures over central South Africa, Botswana, Madagascar, Zimbabwe and South East Indian Ocean are not similar to the geopotential height anomalies of a canonical El Niño pattern. The negative geopotential height anomalies in the South Atlantic Ocean (south of 24ºS) and higher than normal anomalies over the subcontinent in January 2015 are following a canonical El Niño pattern, while the lower than normal pressures anomalies in the Madagascar and higher than normal pressure at central South Africa are not expected.

The negative geopotential height anomalies in the South Atlantic Ocean (south of 24ºS) and higher than normal anomalies over the subcontinent in January 2015 are following a canonical El Niño pattern, while the lower than normal pressures at the Madagascar and higher than normal pressure at central South Africa are not expected during El Niño. During February 2015 (Figure 12c), the lower than normal pressure at the eastern side of southern Africa intensified while higher than normal pressure in the South Atlantic Ocean weakened as December 2016 (Figure 13a) mimics the canonical El Niño pattern over the subcontinent, but the higher than normal pressure has spread across the entire Indian Ocean. January 2016 (Figure 13b) mimics the canonical El Niño pattern events but the lower than normal pressure has shifted towards the Indian Ocean and higher than normal pressures cover the whole subcontinent. February 2016 (Figure 13c) pattern follows the circulation pattern similar to February 2015 with lesser intensity in negative pressures. Finally, March 2016 (Figure 13d) differs from March 2015, due to enhanced positive pressure at the western coast of South and stronger negative pressures that infiltrates the interior.

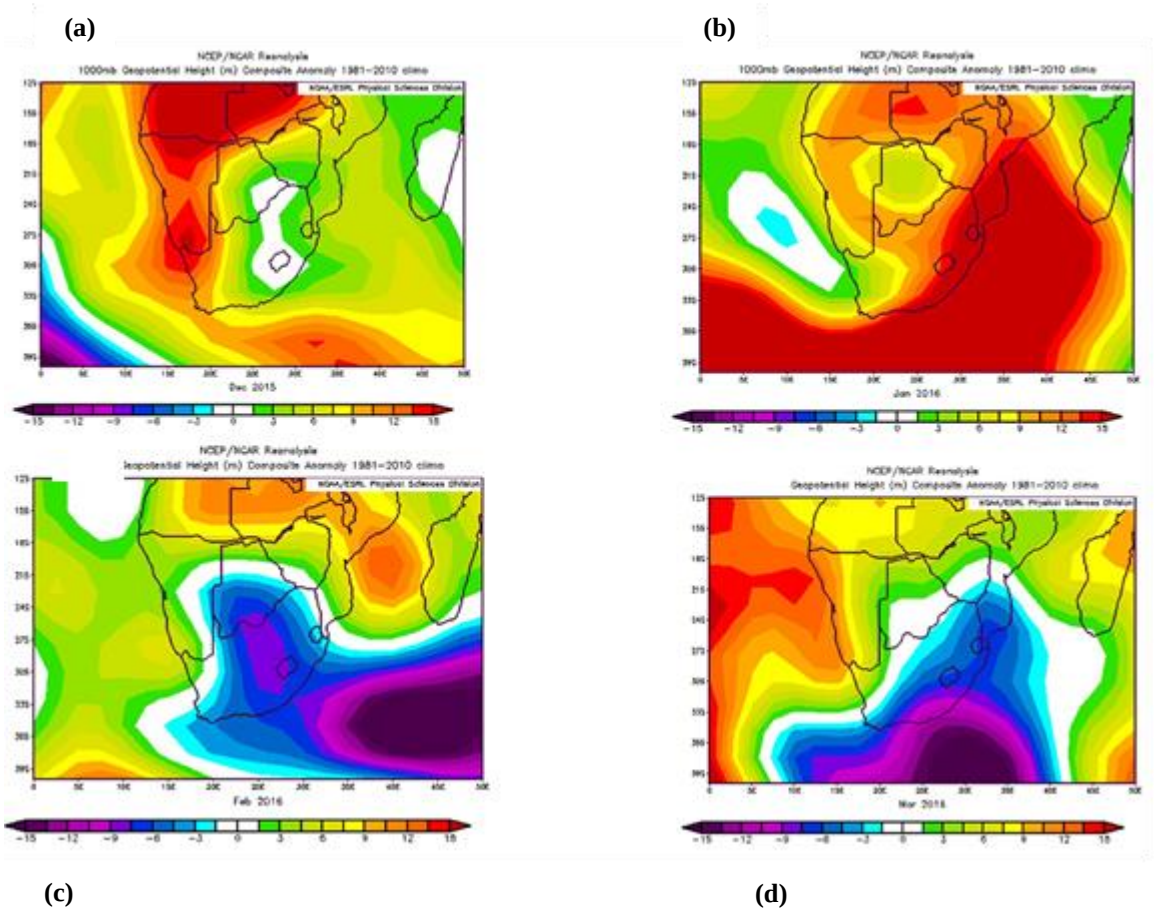

Figure 13: Geopotential height anomalies (m) during summer season (December 2015- March 2016) over southern African at 1000 hPa. (a) December 2015, (b) January 2016, (c) February 2016 and (d) March 2016.

4.4. Geopotential height at 500 hPa

The composite of geopotential height anomalies at 500h Pa (Figure 14) of the canonical El Niño shows positive pressure anomalies over the subtropical and tropical regions across the globe, while negative pressure anomalies are found at lower latitudes. This would help to suppress rainfall above southern Africa. According to Dieppois et al. (2015) such anomalies at the mid-tropospheric level are also associated with an increase in pressure gradient over a substantial part of the Southern Hemisphere and is therefore associated with the increase in westerly wind brushing off southern Africa. The westerly winds (evident at Appendix B) would suppress south- easterly wind in the south Benguela upwelling regions generating warm SST anomalies at the coast. Furthermore, Figure 14 displays a Rossby wave train characterised by the cyclonic anomalies over the South Pacific Ocean extending into the south Atlantic. According to Reason and Phaladi (2005), this Pacific-South American pattern acts together with higher pressure anomalies at upper and lower tropospheric levels to suppress convection over the north-east South Africa and the neighbouring regions.

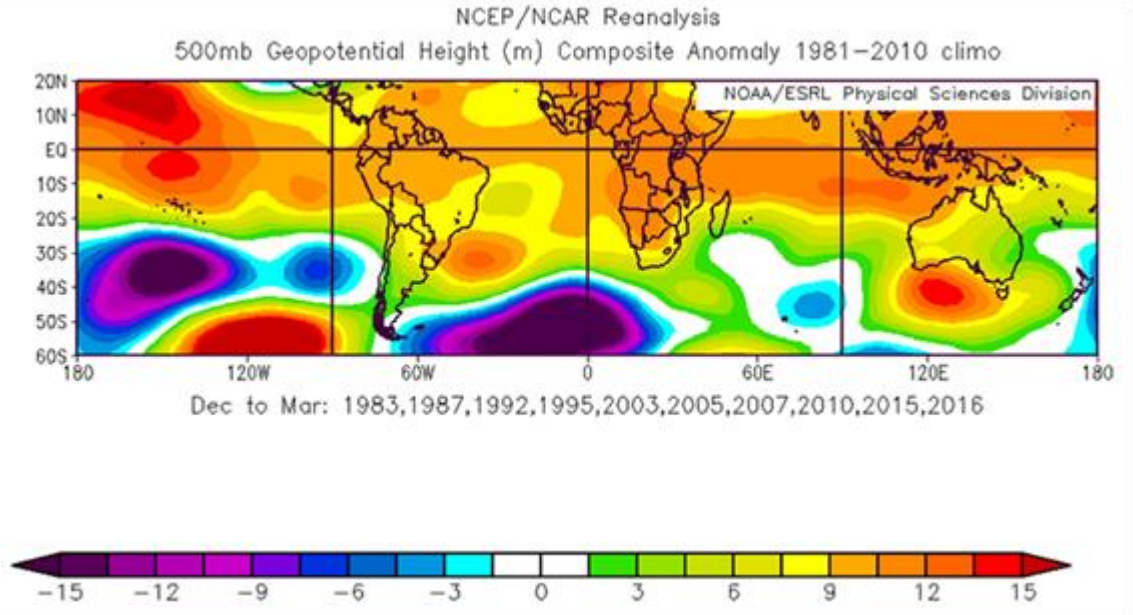

Figure 14: The composite anomaly for geopotential height for El Niño summers at 500 hPa. Positive anomalies imply higher than normal pressure while negative anomalies imply lower than normal pressure. El Niño years considered were 1983, 1987, 1992, 1995, 2003, 2005,2007, 2010, 2015 and 2016.

.

Figure 15 (a), (b) and (c) shows the composite anomaly of geopotential height over southern Africa during El Niño, 2014/2015 and 2015/2016 summers, respectively. Higher than normal pressures are found over the entire southern Africa, except for the lower than normal pressures in the south-western Atlantic and normal pressures south of Madagascar (Figure 15a). The only similar features to canonical El Niño displayed by the summer 2014/2015 at 500 hPa (Figure 15b) geopotential pattern is the higher than normal pressure over the interior. Lower than normal pressures found over southern Madagascar and South Africa differs from the canonical El Niño pattern. Furthermore, intensified 500 hPa geopotential anomalies are observed over western Namibia and western Angola during 2014/2015. During summer 2015/ 2016 (Figure 15c), the pressure patterns mimic that of a canonical El Niño event, except that the higher than normal pressure is covering the entire subcontinent.

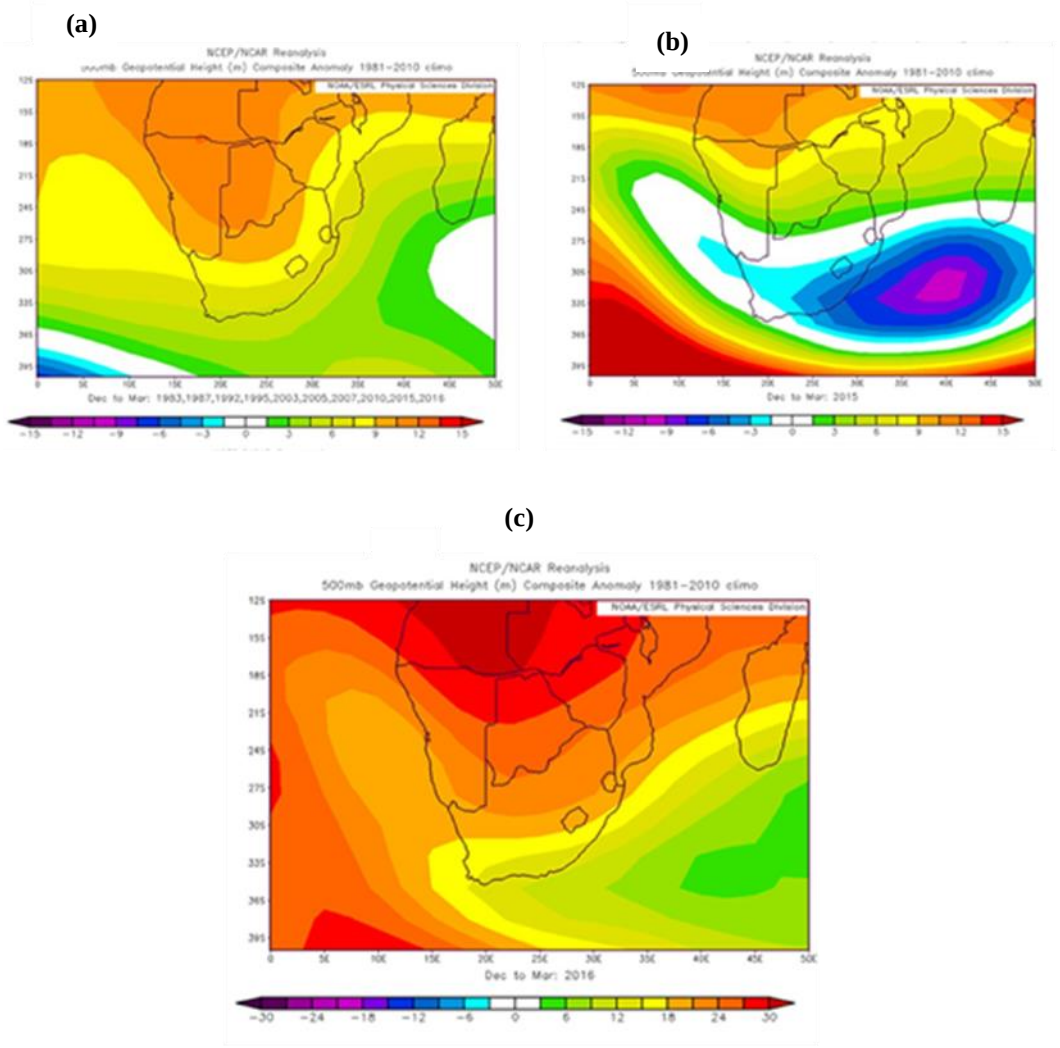

Figure 15 : Geopotential height anomalies (m) during summer season (December 2015-March 2016) over southern African at 500 hPa. (a) December 2015, (b) January 2016, (c) February 2016 and (d) March 2016

Figure 16 shows monthly 500 geopotential anomalies during the summer season of 2014/2015 over southern Africa while Figure 17 shows the same but during the summer of 2015/2016 at 500 hPa. During the December 2015 (Figure 16 a) normal pressures are found over the interior of the subcontinent which is peculiar to an El Niño pattern but December 2016 (Figure 17 a) mimics the pressure pattern very well with increased magnitude over southern Africa. The January of 2015 and 2016 mimics the higher than normal pressures over the interior experienced during a canonical El Niño.

February 2015 (Figure 16c), is characterised by a large cyclonic anomaly over the interior while February 2016 (Figure 17c) is still mimicking the canonical El Niño pattern. However, the western side of the subcontinent is covered by normal pressure and the south-east ocean with lower pressure. Both the pressure patterns during March 2015 (Figure 16d) and 2016 (Figure 17d) do not mimic the canonical El Niño pattern, South Africa during March 2015 has normal pressures while the western side of South Africa is covered by a cyclonic anomaly. This led to normal rainfall over southern Africa. In summary, the large cyclonic anomaly found over the continent during the summer season of 2014/2015 can be attributed to lower to normal pressure conditions of February 2015 and March 2015. While the large anti-cyclonic

anomaly evident on the summer of 2015/2016 can be associated with the higher than normal pressure anomalies during December 2015 and January 2016.

.

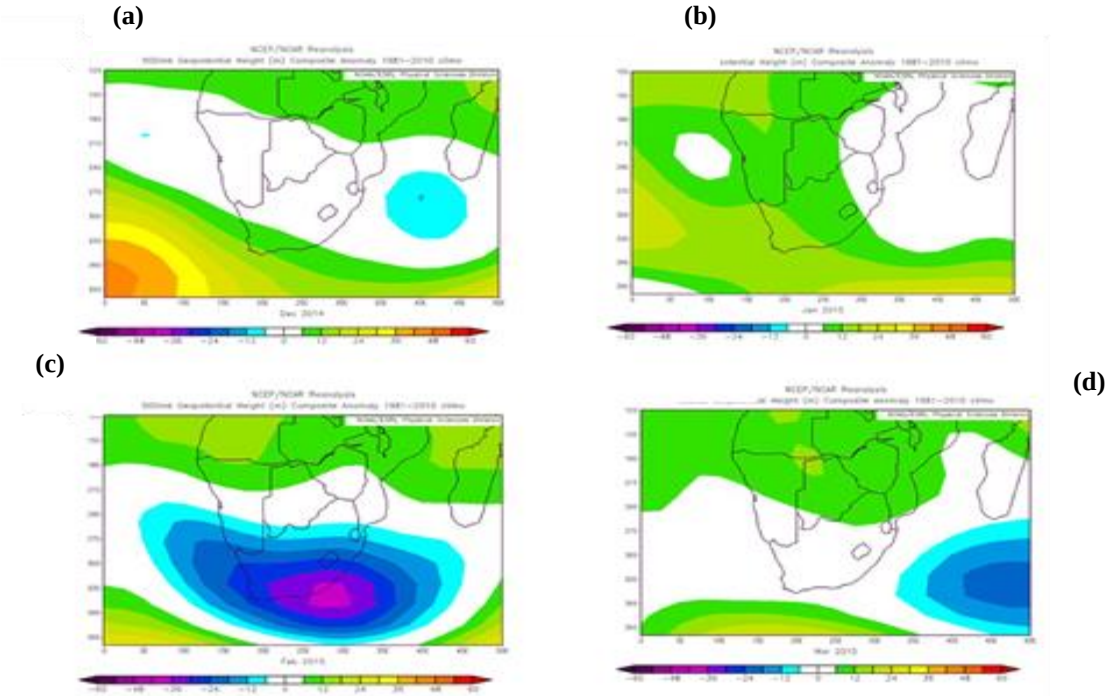

Figure 16 : Geopotential height anomalies (m) during the 2014/2015 summer season over southern Africa at 500 hPa. (a)December 2014, (b) January 2015, (c) February 2015 and (d) March 2015.

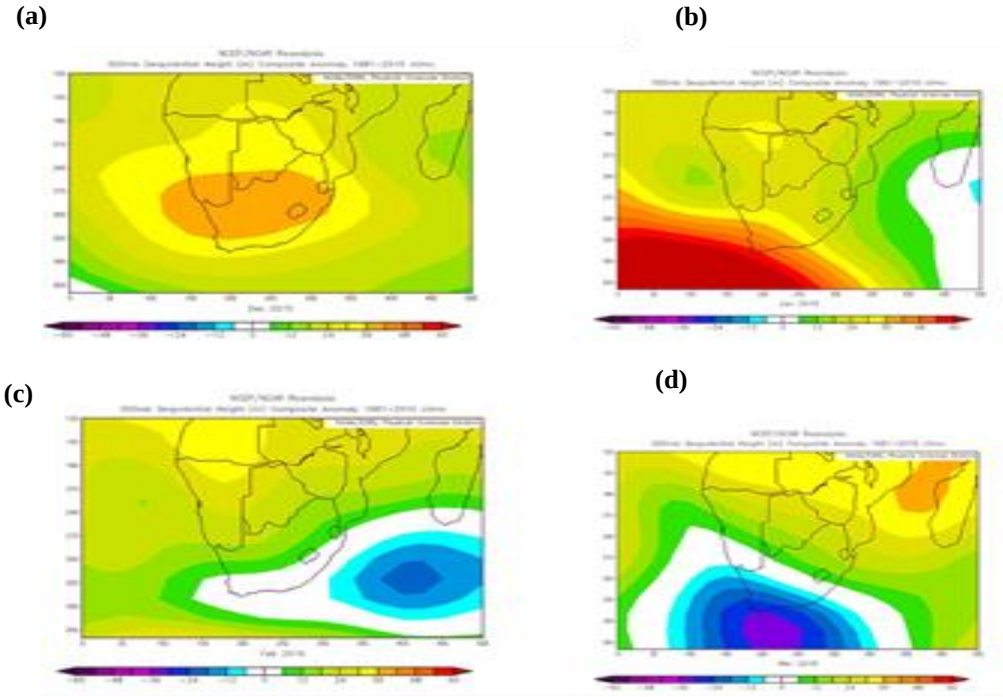

Figure 17: Geopotential height anomalies (m) during the 2015/2016 summer season over southern African at 500 hPa. (a) December 2015, (b) January 2016, (c) February 2016 and (d) March 2016.

4.5. Rainfall climatology

Figure 18 displays the annual mean rainfall cycle over the 8 homogenous areas, which was calculated by averaging monthly means from 1921 to 2016. The north-western Cape and south-Western Cape are categorised as winter rainfall regions. Both areas experience maximum rainfall during June, but the south-western Cape (Figure 18b) accumulates higher rainfall amounts (76.2 mm/month) as compared to 29.37 mm/month acquired by the northern-Western Cape (Figure 18a). The South Coast receives rainfall throughout the year ranging from 33 to 46 mm/month. The remaining five areas all represent the summer rainfall region of South Africa. The western and southern interiors receive their maximum rainfall during March, with the southern interior at a maximum of 70.72 mm/month. Central Interior (Figure 18f), north-eastern Interior (Figure 18h) and KwaZulu-Natal all receives their maximum rainfall during January. The difference between monthly rainfall during summer and winter is more established over the north- eastern interior while KwaZulu-Natal is the wettest area (maximum of 130 mm/month). Due to the spatiotemporal variability in South Africa, it is necessary to understand the climatology of the 8 rainfall regions listed above, before the SPI can be applied. Additionally, at shorter time scales (less than 3 months), in the regions such as south coast, because the precipitation totals are more similar to SPI, a very small anomaly (shortage of 15 mm) can lead to a drought (large SPI values), which will not be the case of KwaZulu-Natal. Therefore, the SPI makes it more useful to look at drought across the region of different climatology (Hayes et al. 1999; Rouault and Richard, 2003).

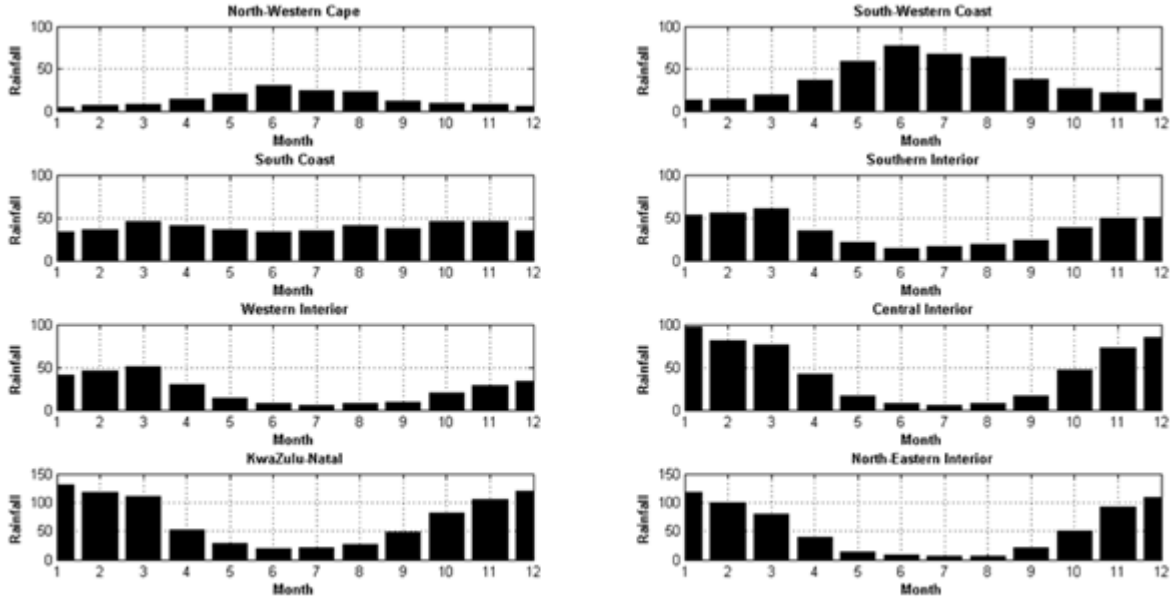

Figure 18: Monthly rainfall mean (mm/month) for the 8-homogenous area defined by SAWS from 1921 to 2016. North- Western Cape (a), South Western Coast (b), South Coast (c), Southern Interior (d), Western Interior (e), Central Interior (f), KwaZulu-Natal (g) ad North-Eastern Interior (h).

4.6. El Niño Index.

To understand the impact of ENSO on the South African droughts, an average Nino 3.4 index from the summer of 1920/1921 to summer 2015/2016 was plotted in Figure 19. Austral summer is usually the season where El Niño reaches its maximum intensity in SST. The index was calculated by averaging the Nino 3.4 index from December to January (DJF) and divided by the standard deviation of that season. Usually, the threshold for categorizing El Niño or La Nina during austral summer for Nino 3.4 SST anomalies is 0.5ºC and this value must be reached for 5 months in a row. Only the average in austral summer will be considered in this study. Therefore, any SST value below -0.5 ºC is classified as La Nina while above + 0.5ºC is classified as an El Niño condition. Based on the Nino 3.4 Index, 24 El Niño and La Nina conditions above and below +/- 0.5º C were chosen from the austral summer of 1920/1921 to 2015/2016. This may be slightly different from El Niño event as defined by agencies in the United States of America but it serves the purpose well enough to define 24 El Niño conditions, 24 La Nina conditions and 46 neutral years. For instance, at the initial stage the summer of 2014/2015 was not classified as El Niño per se by the international community due to the absence of El Niño -like surface winds and convection anomalies (Archer et al., 2017), while our definition does take it as El Niño condition. It was only at later stages upon updated ONI that the summer season of 2014/2015 was classified as a weak El Niño event (http://www.cpc.ncep.noaa.gov/products/analysis_monitoring/ensostuff/ensoyears.shtml).

Out of 94 summer seasons, 24 El Niño conditions occurred during the following summers: 1925/1926, 1930/1931, 1939/1940, 1940/1941, 1941/1942, 1957/1958, 1963/1964, 1965/966, 1968/1969, 1972/1973, 1976/1977,1977/1978, 1982/1983, 1986/1987, 1987/1988, 1991/1992, 1994/1995, 1997/1998, 2002/2003, 2004/005, 2006/2007, 2009/2010, 2014/2015 and 2015/2016. 24 La Niña conditions occurred during the summer of the following years: 1922/1923, 1924/1925, 1931/1932,1933/ 1934, 1937/1938, 1938/1939, 1942/1943, 1945/1946, 1949/1950, 1950/1951, 1953/1954, 1954/1955,1963/1964, 1967/1968, 1970/1971, 1971/1972, 1973/1974, 1975/1976, 1984/1985,1988/1989, 1998/1999, 1999/2000, 2007/2008 and 2010/2011. The three strongest El Niño events occurred during the summer 2015/2016 (1^{st}) 1997/1998 (2^{nd}) and 1982/1983 (3^{rd}). While the strongest La Niña event occurred during the summer season of 1973/1974, followed by 1942/1943 and 1950/1951 being the third strongest La Niña event of the 94-year period. Finally, a protracted El Niño event is evident from the summer years of 1939/1940 to 1941/1942.

Figure 20 shows the time series of droughts at 3 different monthly time scales, i.e. 3, 5 and 17 months over South Africa at the end of February for the 3-month scale and the end of March for the 5-month scale. At a 3-month scale, the values of the SPI reflect short term drought index at the heart of the rainy season, usually used to monitor agricultural drought. At a 5-month scale the SPI values rather reflect most of the rainy summer. The 17 month SPI values rather reflect longer term precipitation anomalies, which affect hydrological systems.

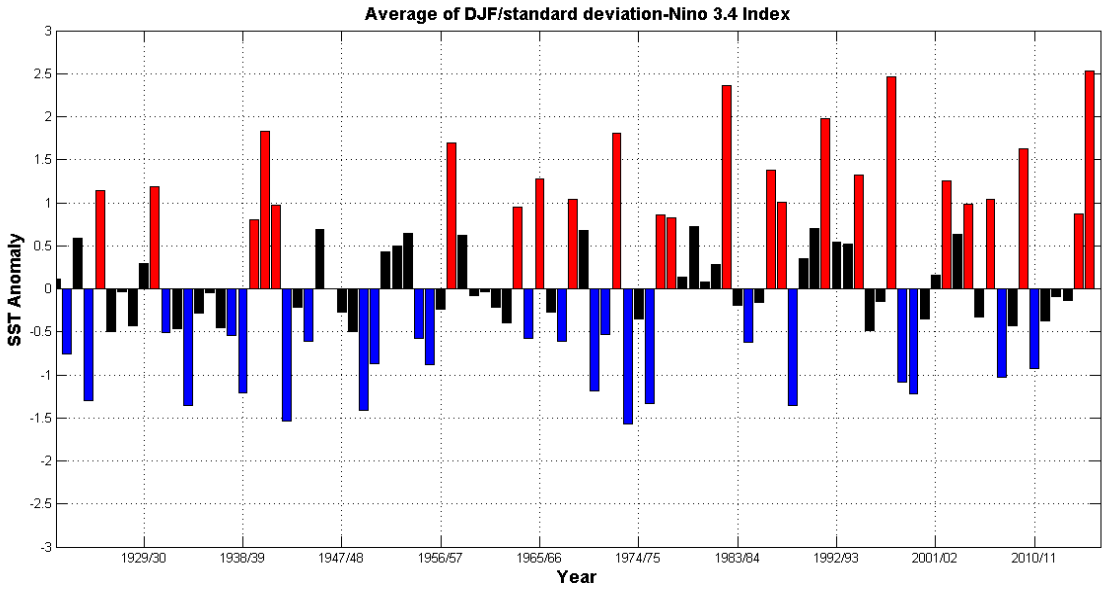

Figure 19 : Nino 3.4 index. Red and blue bars represent El Niño and La Niña respectively, while the black bars represent a neutral year. ENSO episodes are defined from summer of 1921 to 2016.

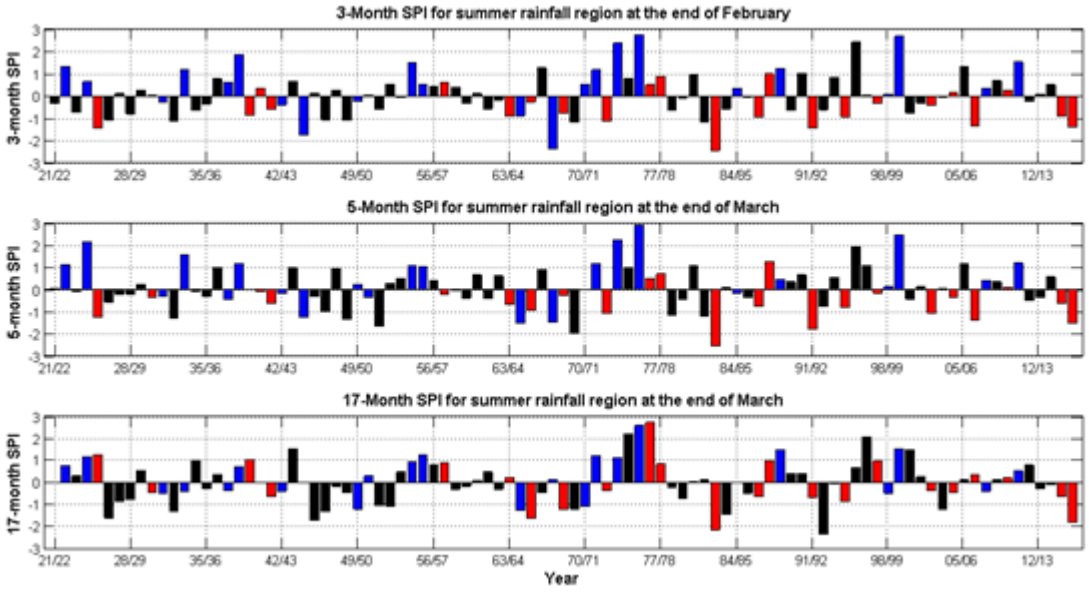

Figure 20: SPI at 3, 5 and 17 month time scale at the end of February for 3 month and March for 5 and 17 month for summer rainfall region.

Rainfall shortage in medium terms and information from this scale can be further be associated with deviation from the means in reservoir level. Table 1 categorises the SPI into different classes, for instance, if a SPI falls within a positive category it indicates that the value is greater than normal, while negative SPI value will indicate that a value is lesser than normal. Furthermore, the negative class of which this paper is dedicated to has a different hierarchy of dryness. SPI value of -2.00 or lesser value classify a drought as extreme; while between -1 and -1.5 a drought will be classified as moderately dry (Table 1).

Table 1: The classification of the SPI values

SPI Class	Drought Category
SPI > 2	Extremely wet
1.50 < SPI ≤ 1.99	Very Wet
1 < SPI ≤1. 49	Moderately Wet
-0. 99 <SPI ≤ 0.99	Near Normal
-1.49 < SPI ≤1.00	Moderately dry
-1.99 < SPI ≤1.50	Severely dry
SPI ≤ -2.00	Extremely dry

Figure 20 further represents the time series of SPI over the summer rainfall region of South Africa, which was averaged over all the summer rainfall sub-regions (Central Interior, KwaZulu-Natal, Northern Interior, Western Interior and Southern Interior). At the 3 and 5- month time scales, South Africa experienced its extreme drought during the El Niño summer of 1982/1993, while at 17-month scale, the driest summer is at 1991/1992. During the strongest El Niño event of 2015/2016, the country experienced its third strongest drought of the century (from 1921 to 2016). It should be further highlighted that after 1970, the relationship between ENSO and southern African rainfall strengthened (Rouault and Richard, 2005, Fauchereau et al., 2003, Richard et al., 2001),

It is also important to note that sometimes El Niño does not lead to drought such as the 1997/1998 and that small El Niño can lead to drought (2014/2015). However, most El Niño events are associated with droughts and most La Niña with wet summer, especially since the 1970s. Since the 1970s, the standard deviation and variations of SPI are bigger from 1940 to 1970s, which confirm the work by Richard et al. (2001) for southern Africa. Sometimes, wet conditions can also occur during El Niño and dry conditions during La Niña. For instance, during the La Niña summer of 1970/1971 at the same monthly time scale, South Africa scored drier than normal conditions. Due to spatiotemporal variability of South African rainfall, it is important to investigate the impact of rainfall within different summer rainfall regimes in the country; therefore, the following subsection will serve this purpose for a 94-year period.

4.7. South African subdomains and SPI

In central interior (Figure 21), the worst dry year at a 3-month scale occurred during La Nina summer of 1967/1968. During the same year, wetter conditions were found over the area at a 17-month time scale, which represent two consecutive seasons. At a 5-month scale, the central interior received its worst drought (>- 2) during the El Niño summer of 1991/1992, while at the 17 months scale the most severe drought at this scale followed a summer after the El Niño event of 1991/1992.

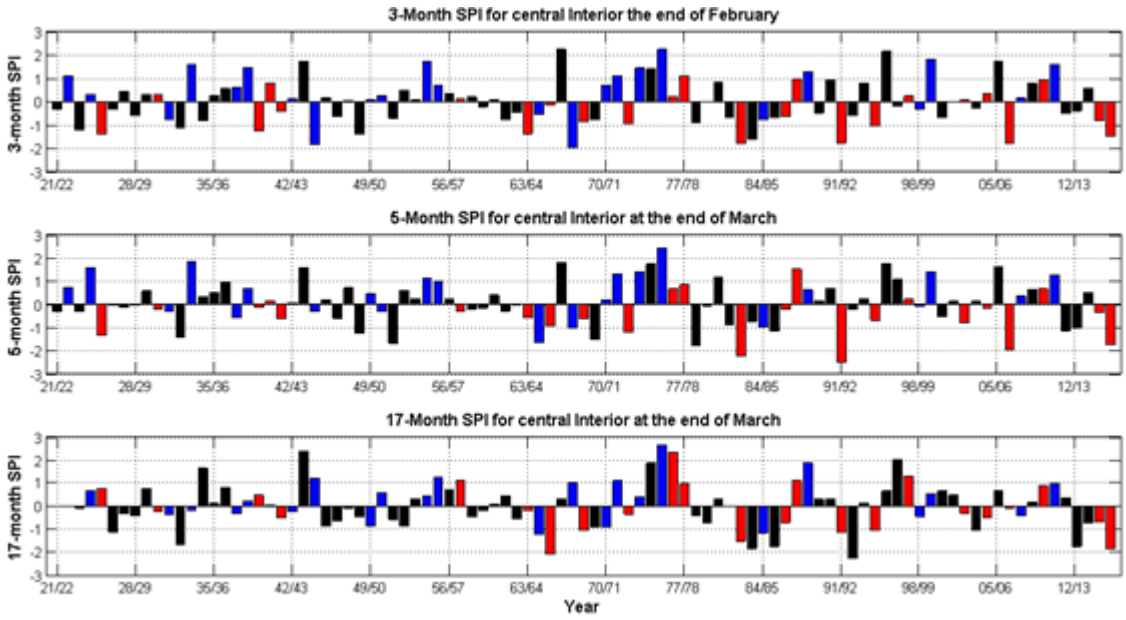

Figure 21: SPI at 3, 5 and 17-months' time scale at the end of February for 3 month and March for 5 and 17 months for Central Interior.

The worst drought at a 3 and 5-months' time scale over KwaZulu-Natal (Figure 22) occurred during the El Niño event of 1982/1983 while the strongest drought at a 17-month scale occurred during the strongest El Niño year of the century in 2015/2016. It is interesting to note that at the 17-months scale, the two strongest wettest events were recorded during the El Niño years of 1977/1978 and 1987/1988. This is because 1976/1977 was slightly above normal but the preceding year was a very wet La Niña year.

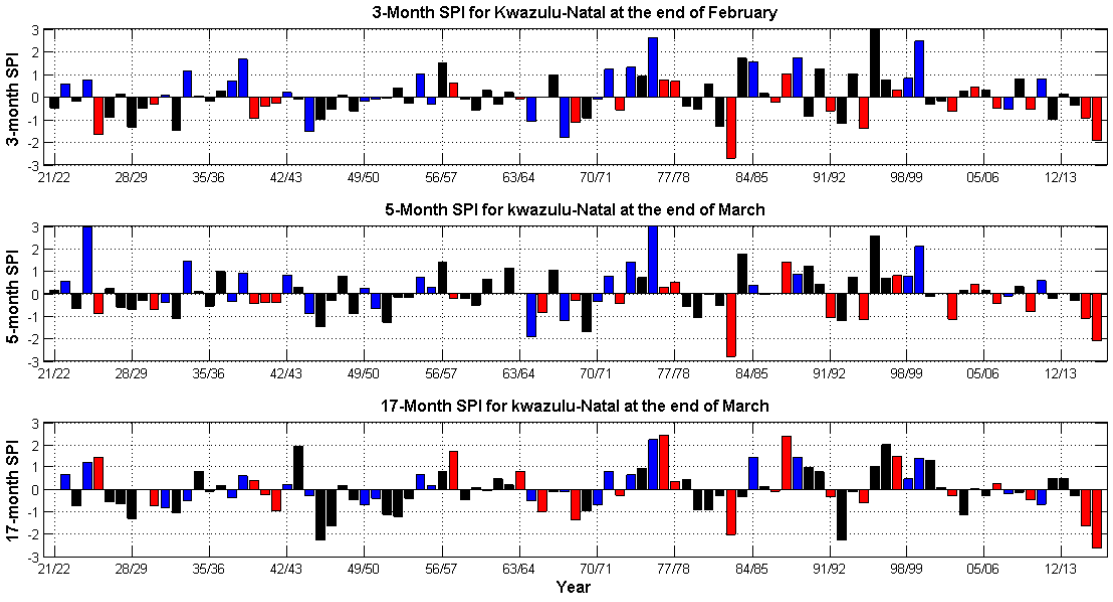

Figure 22: SPI at 3, 5 and 17-month time scale at the end of February for 3 month and March for 5 and 17-months for KwaZulu- Natal.

Over the north-eastern (Figure 23) interior of South Africa the driest summer since 1920/1921 on a 3 and 17-month scale was recorded during the El Niño event of 1982/1983 while at a 5-month scale is recorded during the weak warm Pacific event of 2002/2003. It should be further noted that after 1970s, the frequency and the magnitude of the drought at this region is more pronounced than any sub-region within the South African subdomain.

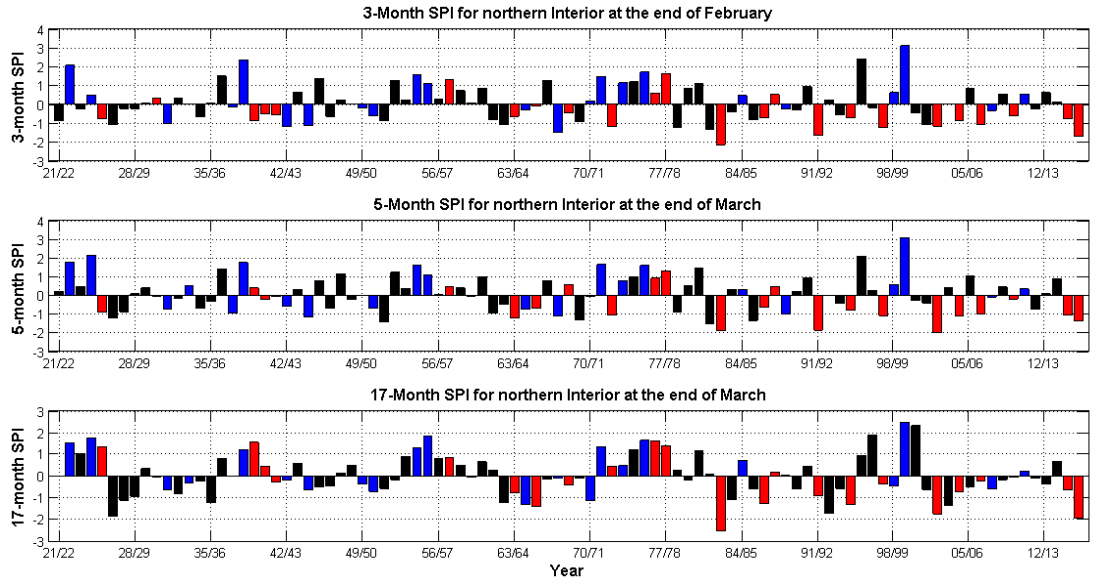

Figure 23: SPI at 3, 5 and 17-month time scale at the end of February for 3 month and March for 5 and 17 month for northern Interior

At the southern interior area (Figure 22) of South Africa, the pattern is very distinctive from the other summer rainfall regions of South Africa, for instance the intensity and frequency of drought has decreased since the 1970s, especially at a 17-month time scale which is opposite from what has happened in southern Africa (Fauchereau et al., 2003, Rouault and Richard 2003, 2005). However, the worst drought since 1921/1922 in this region at the 3 and 5-month scale occurred after the 1970s during the 1982/1983 El Niño event. At a 17-month scale, it is notable that a severe drought occurred during the normal year of 1945/1946 following two below normal but not exceptionally below normal season summer season while the wettest summer is recorded during the El Niño year of 1976/1977. Furthermore, it is also very interesting to note that during the strongest El Niño event of the century 2015/2016, the area had normal to near normal SPI values at all scales.

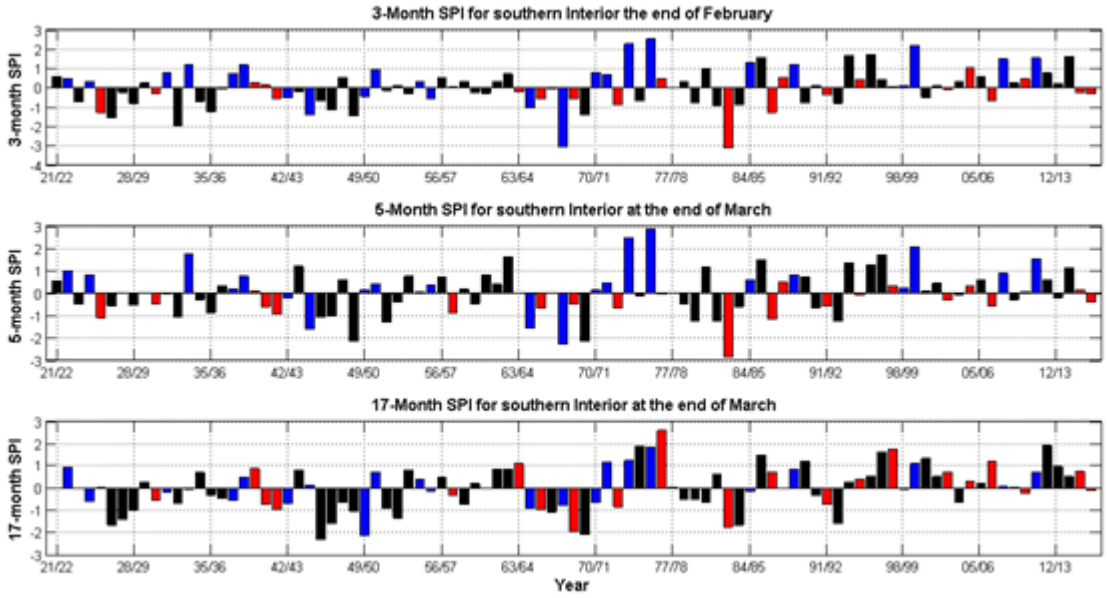

Figure 24: SPI at 3, 5 and 17-months' time scale at the end of February for 3 month and March for 5 and 17-month for southern Interior.

Over the western interior (Figure 25) of South Africa it is notable that all the driest years were recorded during neutral years at 3, 5 and 17-month time scales during the following summers respectively: 1967/1968, 1932/1933 and 1992/1993. Note that 1992/1993 followed the 1991/1992 El Niño drought which impacted that region at a 2-year scale. Furthermore, at the 17-month time scale, dry conditions over these regions persisted from the normal summer of 1978/1979 to the El Niño summer of 1986/1987 and these prolonged droughts were relieved during the El Niño summer of 1987/ 1988.

In conclusion, the relationship between drought and El Niño at the regional scale is not as strong as it is for the all summer rainfall. This has some consequences for the seasonal forecast based on past events at the regional scale. Additionally, two of the strongest El Niño events of 1997/1998 and 2015/2016 had different effect on the rainfall of South Africa. For instance, KwaZulu-Natal, the central and western interior of South Africa received normal SPI values for all the timescales during the summer of 1997/1998 while the north-eastern interior of South Africa is the only region within the subdomains that had drought within this second strongest El Niño event. During the strongest El Niño event of 2015/2016, all the subdomains within South Africa had droughts, but it was not the strongest of the 20th and 21st century based on the 94-year period. KwaZulu-Natal is the only subdomain within South Africa to record 2015/2016 as the driest year of the record but at 17-month scale.

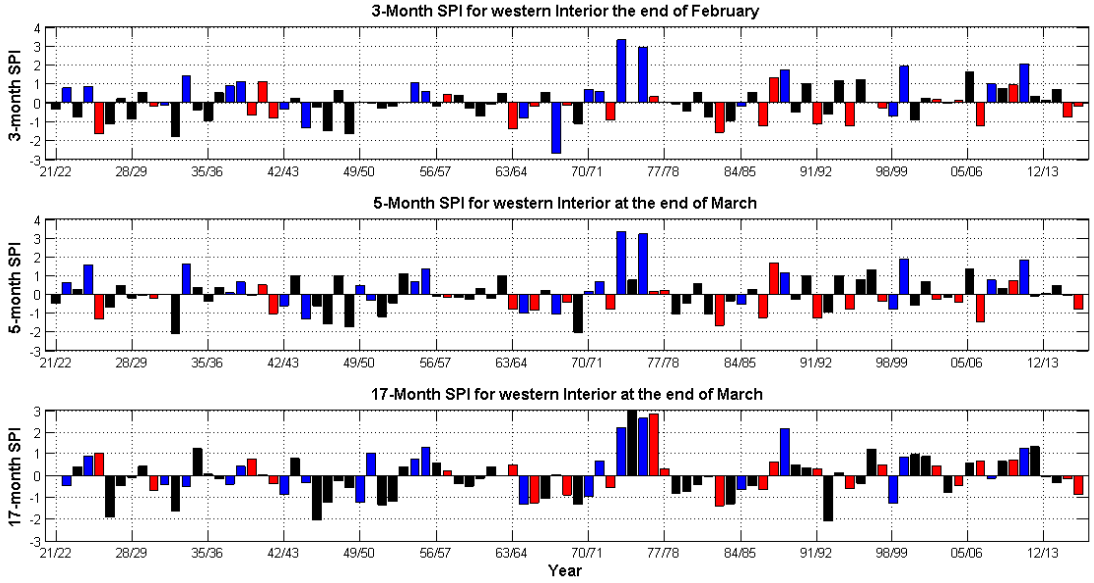

Figure 25: SPI at 3, 5 and 17-month time scale at the end of February for 3 month and March for 5 and 17 months for western Interior

5. Conclusion

The first objective of the study was to investigate the oceanic and atmospheric conditions associated with droughts that occurred during the austral summer season of 2014/2015 and 2015/2016. Results suggest that the oceanic and atmospheric conditions during the two summers were of a canonical El Niño pattern, especially for 2015/2016, represented by averaging a number of El Niño events together and looking at the difference from climatology. The difference in the variables (rainfall, SST and geopotential height) was due to monthly anomalies that occurred during the distinctive summer rainfall regions. Not all months have the same El Niño pattern and even during El Niño normal rainfall or above normal rainfall can occur during an El Niño summer. This confirms that El Niño event have different signatures in southern Africa at regional scale and also that not all months are dry, even during a very dry season. Same can be said for SST, for instance, there was cooler than normal SST over the Benguela Current system during December 2014 and March 2015. Seasonal cooling over the Mozambique Channel in all the months of the summer seasons and warming of the South Pacific Ocean during January 2015. Those SST pattern are different from canonical El Niño pattern. The cooler than normal SST over South Coast, west coast and Mozambique over the Mozambique Channel during December 2014 and March 2015 could have contributed to seasonal cooling along the Benguela Current System during 2014/2015. The SST anomalies during December 2015 and January 2016 mimic the El Niño pattern very well, but with higher magnitude. It is only the colder than normal SST at south coast during February 2016 and Namibian and west coast during March 2016 that doesn't mimic the canonical El Niño patterns.

At 500 hPa, the large cyclonic anomaly for the average of the summer 2014/ 2015 is peculiar for an El Niño pattern over the subcontinent. It can be attributed to the lower than normal pressure conditions of February 2015 and March 2015. While the large anti-cyclonic anomaly

(canonical El Niño pattern), evident on the summer of 2015/2016 can be associated with the higher than normal pressure anomalies during December 2015 and January 2016.

The second objective of this study was to examine, whether the summer 2015/2016 was the strongest of the century, and the results suggest otherwise, although it is still one of the strongest. Since, the study did not account for the increase in temperature due to global warming; one could argue that 2015/2016 was the strongest drought based on rainfall only. During this strongest El Niño event of 2015/2016, KwaZulu-Natal was the only region to be hit by the strongest drought of the 94-year period since 1921 but at a longer time scale (17 months). There is a little difference between 3 months SPI at the end of February and 5 months SPI at the end of March. To conclude, for South Africa summer rainfall 2015/2016 was the fifth worst drought after the El Niño related drought of 1982/1983 and 1991/1992 and the non-El Niño related drought of 1967/1968 and 1944/1945 at the seasonal month scale. At the 17-month scale, an index that encompasses two summer seasons 2015/2016 was the third worst drought since summer 1921/1922 due to dry conditions in 2014/2015.

Appendix A

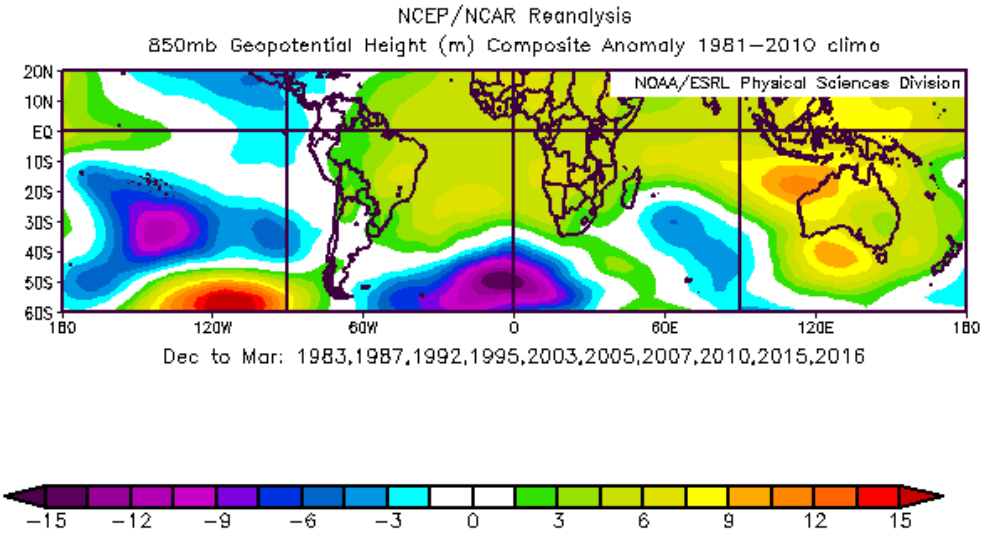

Composite for geopotential height anomaly (m) for the summer season during El Niño years from December 1982 to March 2016 at 850 hPa. Positive anomalies indicate higher than normal pressure and negative anomalies indicate lower than normal pressure. El Niño years considered were 1983, 1987, 1992, 1995, 1998, 2002, 2005, 2007, 2010, 2015.

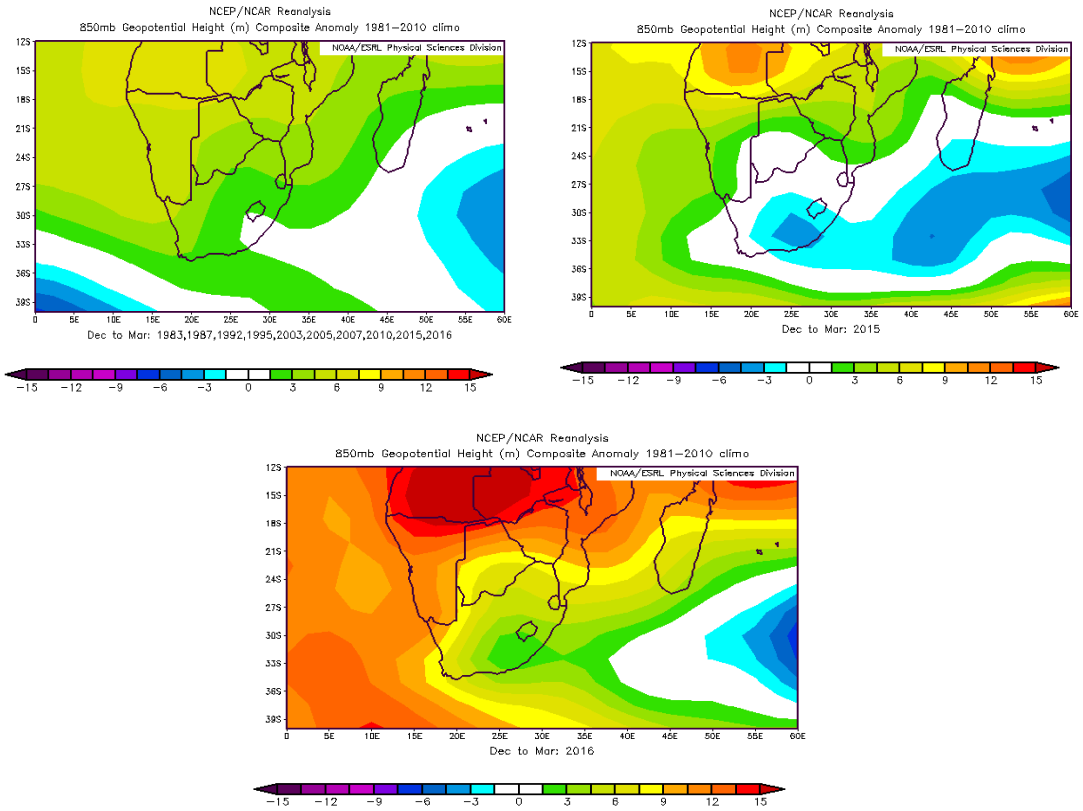

Top left: composite of 850 hPa geopotential height anomaly (m) during El Niño for the summer season Dec 1982 to Mar 2016 for southern African (a), Top right 2014/2015 (b) and bottom 2015/2016 (c). Positive anomalies mean wetter than normal pressure and negative anomalies mean lower than normal pressure.

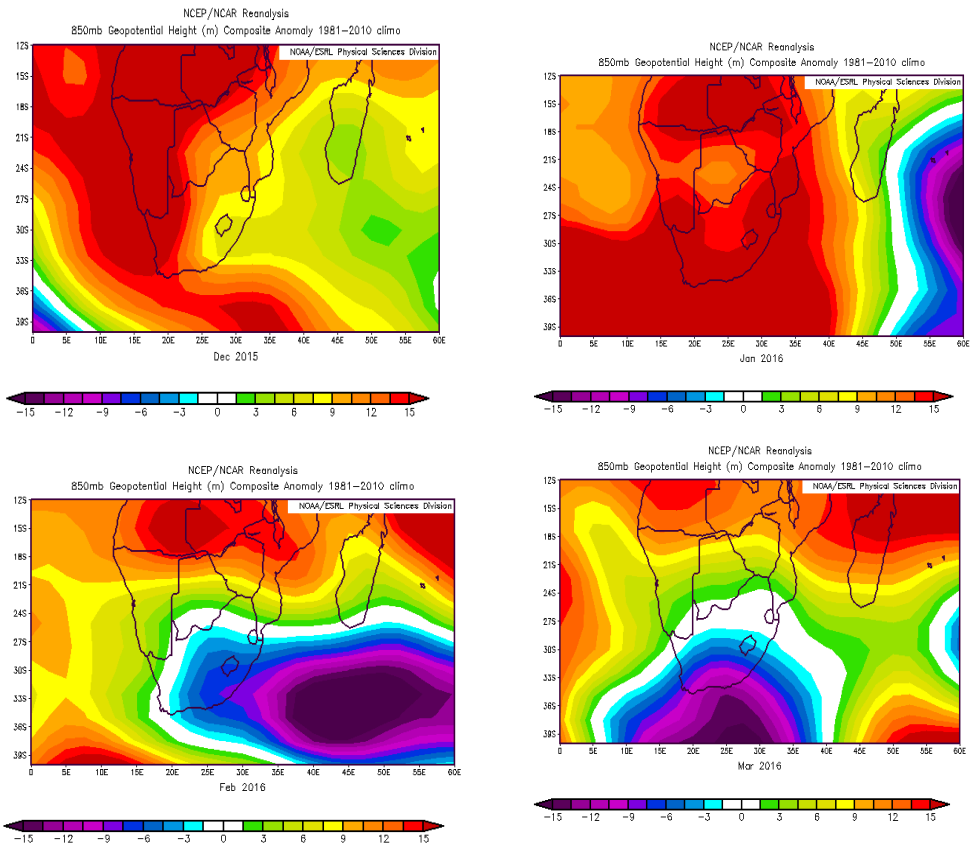

850 hPa geopotential height anomalies (m) during summer season (December 2014-March 2015) over Southern African at 1000 hPa. (a)December 2014, (b) January 2015, (c) February 2015 and (d) March 2015.

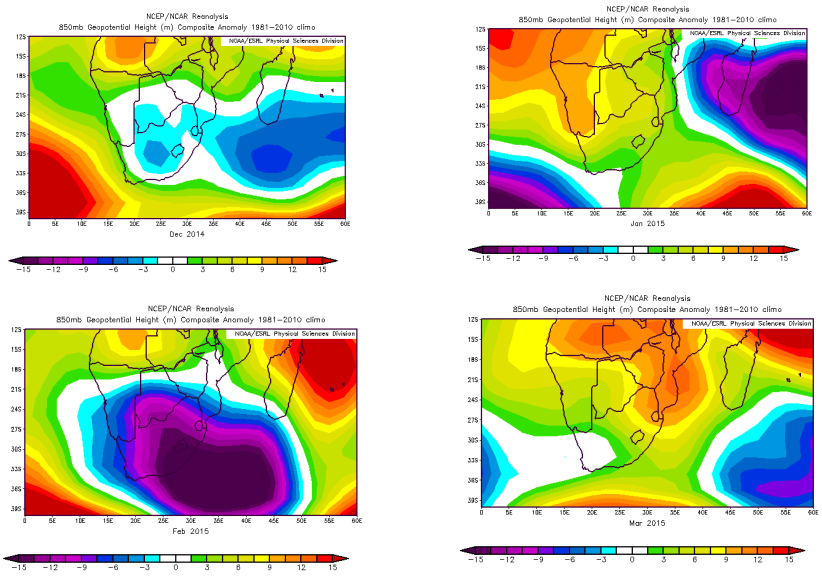

Geopotential height anomalies (m) during summer season (December 2015-March 2016) over southern African at 1000 hPa. (a) December 2015, (b) January 2016, (c) February 2016 and (d) March 2016.

Appendix B

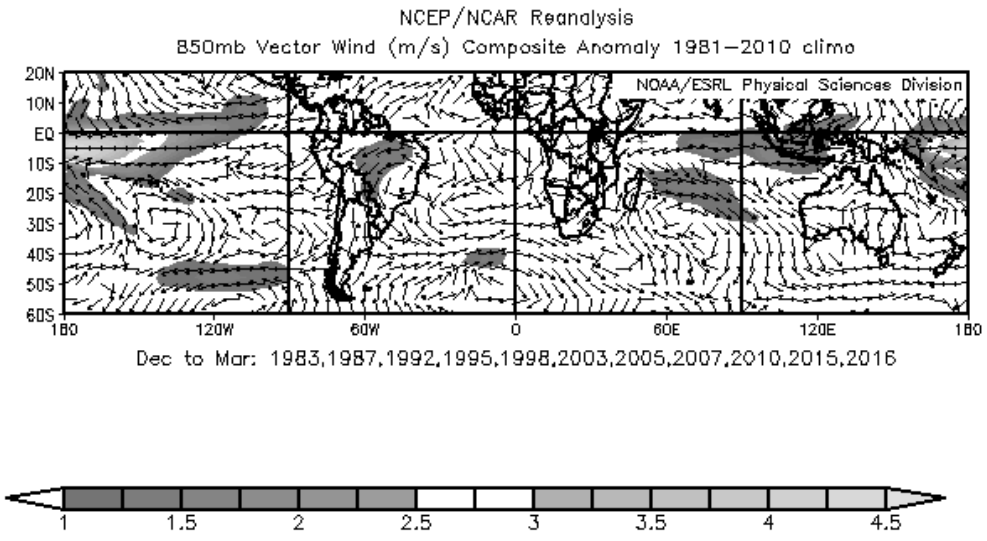

Composite for vector wind (m/s) for the summer season during El Niño years from December 1982 to March 2016 at 1000 hPa. El Niño years considered were 1983, 1987, 1992, 1995, 1998, 2002, 2005, 2007 , 2010, 2015.

References

AgriSA, 2016. “A raindrop in the drought “- Agri SA’s status report on the current drought crisis. February 2016.

Archer, E.R.M., Landman, W.A., Tadross, M.A., Malherbe, J., Weepener, H., Maluleke, P. and Marumbwa, F.M., 2017. Understanding the evolution of the 2014–2016 summer rainfall seasons in southern Africa: Key lessons. *Climate Risk Management*, *16*, pp.22-28.

Awan, J.A., Bae, D.H. and Kim, K.J., 2015. Identification and trend analysis of homogeneous rainfall zones over the East Asia monsoon region. *International Journal of Climatology*, *35*(7), pp.1422-1433.

Behera, S.K. and Yamagata, T., 2001. Subtropical SST dipole events in the southern Indian Ocean. Geophysical Research Letters, 28(2), pp.327-330.

Blamey,R.C., 2012. Mesoscale Convective Complexes over southern Africa (Doctoral dissertation, University of Cape Town).

Blamey, R. C., and Reason, C. J. C. 2013. The role of mesoscale convective complexes in southern Africa summer rainfall. Journal of climate, 26(5), 1654-1668.

Cane, M.A., 2005. The evolution of El Niño, past and future. Earth and Planetary Science Letters, 230(3), pp.227-240.

Crétat, J., Richard, Y., Pohl, B., Rouault, M., Reason, C., and Fauchereau, N. 2012. Recurrent daily rainfall patterns over South Africa and associated dynamics during the core of the austral summer. International Journal of Climatology, 32(2), 261-273.

Cook, K.H., 2000. The South Indian convergence zone and interannual rainfall variability over southern Africa. *Journal of Climate*, *13*(21), pp.3789-3804.

Dai, A., 2011. Drought under global warming: a review. Wiley Interdisciplinary Reviews: Climate Change, 2(1), pp.45-65.

Dieppois, B., Rouault, M., and New, M. 2015. The impact of ENSO on Southern African rainfall in CMIP5 ocean atmosphere coupled climate models. Climate Dynamics, 1-18.

Driver, P. M. 2014. Rainfall variability over southern Africa. (Doctoral dissertation, University of Cape Town).

Dube, L. T., 2002. South African climate. South African Geographical Journal, 48(1), pp.125-138.

Dufois, F., and Rouault, M. 2012. Sea surface temperature in False Bay (South Africa): Towards a better understanding of its seasonal and inter-annual variability. Continental Shelf Research, 43, 24-35.

Fauchereau, N., Pohl, B., Reason, C. J. C., Rouault, M., and Richard, Y. 2009. Recurrent daily OLR patterns in the Southern Africa/Southwest Indian Ocean region, implications for South African rainfall and teleconnections. Climate Dynamics, 32(4), 575-591.

Fauchereau, N., Trzaska, S., Rouault, M., and Richard, Y. 2003. Rainfall variability and changes in southern Africa during the 20th century in the global warming context. Natural Hazards, 29(2), 139-154.

Harrison, M. S. J. 1984. A generalized classification of South African summer rain-bearing synoptic systems. Journal of Climatology, 4(5), 547-560.

Hart, N. C. G., Reason, C. J. C., and Fauchereau, N. 2010. Tropical-extratropical interactions over southern Africa: three cases of heavy summer season rainfall. Monthly weather review, 138(7), 2608-2623.

Hayes, M.J., Svoboda, M.D., Wilhite, D.A. and Vanyarkho, O.V., 1999. Monitoring the 1996 drought using the standardized precipitation index. Bulletin of the American Meteorological Society, 80(3), pp.429-438.

Huffman, G. J., and Bolvin, D. T. 2013. GPCP Version 2.2 SG Combined Precipitation Data Set Documentation.

Hermes, J.C. and Reason, C.J.C., 2005. Ocean model diagnosis of interannual coevolving SST variability in the South Indian and South Atlantic Oceans. Journal of Climate, 18(15), pp.2864-2882.

Lyon, B., 2009. Southern Africa summer drought and heat waves: observations and coupled model behavior. Journal of Climate, 22(22), pp.6033-6046.

Malherbe, J., Dieppois, B., Maluleke, P., Van Staden, M. and Pillay, D.L., 2016. South African droughts and decadal variability. *Natural Hazards*, *80*(1), pp.657-681.

Manatsa, D., Mukwada, G., Siziba, E. and Chinyanganya, T., 2010. Analysis of multidimensional aspects of agricultural droughts in Zimbabwe using the Standardized Precipitation Index (SPI). *Theoretical and Applied Climatology*, *102*(3-4), pp.287-305.

Mason, S.J. and Goddard, L., 2001. Probabilistic precipitation anomalies associated with ENSO. *Bulletin of the American Meteorological Society*, *82*(4), pp.619-638

Mason, S. J., Lindesay, J. A., and Tyson, P. D. 1994. Simulating drought in southern Africa using sea surface temperature variations. WATER SA-PRETORIA-, 20, 15-15.

McKee, T.B., Doesken, N.J. and Kleist, J., 1993, January. The relationship of drought frequency and duration to time scales. In *Proceedings of the 8th Conference on Applied Climatology* (Vol. 17, No. 22, pp. 179-183). Boston, MA: American Meteorological Society.

Meque, A., and Abiodun, B. J. 2014. Simulating the link between ENSO and summer drought in Southern Africa using regional climate models. Climate Dynamics, 44(7-8), 1881-1900.

Mimmack, G.M., Mason, S.J. and Galpin, J.S., 2001. Choice of distance matrices in cluster analysis: Defining regions. *Journal of climate*, *14*(12), pp.2790-2797.

Mulenga, H. M. 1999. Southern African climate anomalies, summer rainfall and the Angola Low (Doctoral dissertation, University of Cape Town).

Mulenga, H. M., Rouault, M., and Reason, C. J. C. 2003. Dry summers over northeastern South Africa and associated circulation anomalies. Climate Research, 25(1), 29-41.

Reason, C. J. C., and Jagadheesha, D. 2005. A model investigation of recent ENSO impacts over southern Africa. Meteorology and Atmospheric Physics, 89(1-4), 181-205
.
Reason, C. J. C., Landman, W., and Tennant, W. 2006. Seasonal to decadal prediction of southern African climate and its links with variability of the Atlantic Ocean. Bulletin of the American Meteorological Society, 87(7), 941-955

Reason, C. J. C., and Mulenga, H. 1999. Relationships between South African rainfall and SST anomalies in the southwest Indian Ocean. International Journal of Climatology, 19(15), 1651-1673.

Reason, C.J.C., 2001. Subtropical Indian Ocean SST dipole events and southern African rainfall. Geophysical Research Letters, 28(11), pp.2225-2227.

Reason, C. 2015. Tropical South East Atlantic Warm Events and Associated Rainfall Anomalies over southern Africa. Frontiers in Environmental Science, 3, 24.

Reason, C.J.C. and Phaladi, R.F., 2005. Evolution of the 2002-2004 droughtover northern South Africa and potential forcing mechanisms. *South African journal of science*, *101*(11-12), pp.544-552.

Reason, C. J. C., and Rouault, M. 2002. ENSO-like decadal variability and South African rainfall. Geophysical Research Letters, 29(13), 16-1.

Reynolds, R. W., Rayner, N. A., Smith, T. M., Stokes, D. C., and Wang, W. 2002. An improved in situ and satellite SST analysis for climate. Journal of climate, 15(13), 1609-1625.

Richard, Y., Fauchereau, N., Poccard, I., Rouault, M., and Trzaska, S. (2001). 20 th century droughts in southern Africa: spatial and temporal variability, teleconnections with oceanic and atmospheric conditions. International Journal of Climatology, 21(7), 873-885.

Richard, Y., Trzaska, S., Roucou, P., and Rouault, M. 2000. Modification of the southern African rainfall variability/ENSO relationship since the late 1960s. Climate Dynamics, 16(12), 883-895.

Rouault, M., Florenchie, P., Fauchereau, N., and Reason, C. J. 2003. South East tropical Atlantic warm events and southern African rainfall. Geophysical Research Letters, 30(5).

Rouault, M., Pohl, B., and Penven, P. 2010. Coastal oceanic climate change and variability from 1982 to 2009 around South Africa. African Journal of Marine Science, 32(2), 237-246.

Rouault, M., and Richard, Y. 2003. Intensity and spatial extension of drought in South Africa at different time scales. Water SA, 29(4), 489-500.

Rouault, M. and Richard, Y., 2005. Intensity and spatial extent of droughts in southern Africa. *Geophysical Research Letters*, *32*(15).

Rouault, M., Roy, S. S., and Balling, R. C. 2013. The diurnal cycle of rainfall in South Africa in the austral summer. International Journal of Climatology, 33(3), 770-777.

Peters, E. 2003. Propagation of drought through groundwater systems - Illustrated in the Pang (UK) and Upper-Guadiana (ES) catchments. Ph.D. thesis. Wageningen University.

Philippon, N., Rouault, M., Richard, Y., and Favre, A. 2012. The influence of ENSO on winter rainfall in South Africa. International Journal of Climatology, 32(15), 2333-2347.

Tyson, P. D., and Preston-Whyte, R. A. 2000. Weather and climate of southern Africa. Oxford University Press.

Ujeneza, E.L. and Abiodun, B.J., 2015. Drought regimes in Southern Africa and how well GCMs simulate them. *Climate Dynamics*, *44*(5-6), pp.1595-1609.

Usman, M.T. and Reason, C.J.C., 2004. Dry spell frequencies and their variability over southern Africa. *Climate Research*, *26*(3), pp.199-211